# DEVELOPMENT AND VALIDATION OF LARGE-SIZED ENGINEERED CARTILAGE CONSTRUCTS IN FULL –THICKNESS CHONDRAL DEFECTS IN A RABBIT MODEL

by

Jillian Maureen Brenner

A thesis submitted to the Department of Chemical Engineering

In conformity with the requirements for

the degree of Master of Applied Science

Queen's University

Kingston, Ontario, Canada

(January, 2012)

Copyright ©Jillian Maureen Brenner, 2012

# Abstract

Long-term applicability of current surgical interventions for the repair of articular cartilage is jeopardized by the formation of mechanically inferior repair tissue. Cartilage tissue engineering offers the possibility of developing functional repair tissue, similar to that of native cartilage, enabling long-lasting repair of cartilage defects. Current techniques, however, rely on the need for a large number of cells, requiring substantial harvesting of donor tissue or a separate cell expansion phase. As routine cell expansion methods tend to elicit negative effects on cell function, the following study describes an approach to generate large-sized engineered cartilage constructs ($\geq 3$ $cm^2$) directly from a small number of immature rabbit chondrocytes (approximately 20,000), without the use of a scaffold. After characterizing the hyaline-like engineered constructs, the *in vivo* repair capacity was assessed in a chondral defect model in the patellar groove of rabbits.

*In vitro* remodeling of the constructs developed in the bioreactor occurred as early as 3 weeks, with the histological staining exhibiting zonal differences throughout the depth of the tissue. With culturing parameters optimized (3 weeks growth under 15 mM $NaHCO_3$), constructs were grown and implanted into critical-sized 4 mm chondral defects. Assessed after 1, 3 and 6 months ($n=6$), implants were scored macroscopically to evaluate integration and survival of the implants. Out of 18 rabbits, 16 received normal or nearly normal over-all repair assessment. Histological and immunohistochemical evaluation showed good integration with surrounding cartilage and underlying subchondral bone. Architectural remodeling of the constructs was present at each time

point, with the presence of flattened chondrocytes at the implant surface and columnar arrangement of chondrocytes in deeper zones. The observation of *in vivo* remodeling was also supported by the changes in biochemical composition of the constructs. At each time point, constructs had a collagen to proteoglycan ratio similar to that of native cartilage (3:1 collagen to proteoglycan). In contrast, the repair tissue for each control group was inferior to that produced with treated defects. These initial results hold promise for the generation of engineered articular cartilage for the clinical repair of cartilage defects without the limitations of current surgical repair strategies.

## Acknowledgements

I have been fortunate throughout my Master's to have been supported and encouraged by a number of individuals. I would like to express my gratitude to Dr. Stephen Waldman for giving me the opportunity to delve into the world of engineering. Through his guidance I have stayed the course on my two-year (and a half) quest to unlock Prometheus' secret of regeneration.

Along the way I have been lucky to have found many people who have graciously donated their time to my research. A very special thanks goes out to Dr. Stephen Pang and Dr. Yat Tse, I would not have been able to embark on such an ambitious animal model study without their help, guidance and patience. Other invaluable participants in my project include Dr. Andrew Winterborn, Dr. Janine Handforth, Dr. Davide Bardana and especially Debbie Harrington. Although I never got used to using rabbits in my research, I was comforted by the fact that they had Debbie as their caretaker.

I feel lucky to have been a part of the J crew…James, Justin (honorary members include Jenna and Jackie, downgraded to honorary as you guys left us behind). I spent as much time laughing with you guys in the lab as I did in our time off- including the hilarious time when Justin shot himself in the leg with a BB gun!

I am also fortunate to have been part of the Waldman lab. Dull moments in the lab were few and far between with Jake, Denver, Renata, Kathleen and Joanna around…quiet moments non-existent with me around. And I also like to consider myself a part-time

student of the Pang lab. Bench space was scarce but they always welcomed me into their lab on dissection days and IHC staining days.

Although I may not miss the town that stole my car, I will deeply miss the amazing friends I have met there. Joanne and Katie have been there with me from my initial biochemistry days to my Master's degree. For better or worse, we have stuck it out in academia life at Queen's University.

I am lucky to have many wonderful friends in my life. A special shout out to Roxanne, Chris and Stella for giving Charlie and me a home while I finished up my thesis. I would also like to thank Aydin for welcoming me into his and Amanda's home and Amin for his encouragement when I was writing in Ottawa.

Amanda May Beaubien, your support and friendship have never faltered. I am lucky to call you my best friend and I can only hope to pay you back someday for all your help!

And last but definitely not least I would like to thank my amazing family for their continual support and understanding. I am truly lucky to have parents and a brother who believe in me and won't let me settle for anything less than I deserve.

# Statement of Contributions

The surgeries for the first study were performed by Dr. Davide Bardana (Department of Surgery, Queen's University, Kingston, Canada) and the surgeries for the second study were performed by Dr. Stephen Pang (Department of Biomedical and Molecular Science, Queen's University, Kingston, Canada). Post-surgical animal care and handling was performed by Debbie Harrington (Queen's veterinary services). The generation of rapid-prototyped molds of imaged joint surfaces and the surface morphology measurement was conducted by Dr. Manuela Kunz (Human Mobility Research Centre, Kingston General Hospital and Queen's University, Kingston, Canada). Macroscopic scoring was performed with Dr. Yat Tse (Department of Biomedical and Molecular Science, Queen's University, Kingston, Canada) and ICRS II histological scoring was performed by Dr. Mark Hurtig (Clinical Studies, University of Guelph, Guelph, Ontario).

# Table of Contents

# List of Figures

# List of Tables

# Chapter 1

# Introduction

## 1.1 Articular Cartilage Injury and Degradation

Although deceptively simple in its composition, articular cartilage plays a vital role in enabling body movement. Located within diarthrodial joints, in which it encases and protects the underlying subchondral bone, articular cartilage enables almost frictionless coordination of the joint[1]. The poor regenerative capacity of this remarkable tissue is not a recent discovery. In 1743 William Hunter noted that cartilage "once destroyed, is not repaired"[2]. Ideally this occurrence would be of no consequence, as articular cartilage is designed to provide eight decades worth of normal joint activity[3]. But in individuals afflicted with articular cartilage injury or disease, this limited repair capacity can lead to altered or even total loss of joint function.

Osteoarthritis (OA) is a common musculoskeletal disease and involves the erosion of articular cartilage in diarthrodial joints. Individuals with OA experience pain and disability due to a progressive degeneration of cartilage. In severe cases this can ultimately result in total loss of joint function[4,5]. OA can be found in every country and is a significant source of economic and social burden. An estimated 27 million people currently suffer from OA in the United States. This number translates into approximately 500,000 joint replacements every year and $60 billion spent on direct and indirect costs[4,6].

## 1.2 Articular Cartilage Repair Strategies

In response to injury, chondrocytes (the singular cell population in articular cartilage) will start to proliferate, all the while increasing their matrix production. Counter-intuitively, these cells and newly-synthesized matrix do not fill in the tissue defect, eventually failing to restore the damaged tissue[3,7]. Another repair response can occur when the defect penetrates into the underlying bone (osteochondral defect), allowing blood and other exogenous factors into the defect area[8]. Unlike normal hyaline cartilage, that is specific to articular joints, the generated repair tissue is a fibrous cartilage, ill-suited to the mechanical environment in the joint. These repair responses are generally short-lived and will be influenced by a variety of factors, including patient's age, activity level, defect size and type [8,9].

The development of clinical therapies for cartilage repair has proven to be a challenging task. Our limited knowledge of articular cartilage's ability for self-repair is compounded by our inability to determine the exact causes of cartilage injury or disease, including the etiology of OA[10,11,12]. Current therapeutic strategies include: i) rinsing or removal of free bodies from the joint (lavage and debridement), ii) increasing articular cartilage's intrinsic repair capacity (abrasion arthroplasty, drilling and microfracture), iii) resurfacing of the defect with grafts (mosaic arthroplasty) or cells (autologous chondrocyte implantation) and iv) total joint replacement[9].

The rationale behind joint lavage and debridement is the promotion of pain relief, rather than restoration of joint function. Lavage is the rinsing of the joint surface with a solution, whereas debridement involves lavage, as well as excision of damaged or diseased cartilage[9]. Strategies to increase cartilage's ability for self-repair were developed in response to the observed healing response with osteochondral defects. In a clinical setting, these techniques are characterized by variable results and rely heavily on multiple factors (age, size/location of defect)[9,1].

Resurfacing of defect areas with cells or graft tissue dates back to the mid-nineties and is still commonly employed in clinical trials[13,14]. Mosaic arthroplasty involves the harvesting and implantation of cartilage/bone plugs into the defect site. Autografts are harvested from a low-weight bearing region of the patient's joint, eliminating immunogenic responses that can lead to graft rejection[5,9]. Alternatively, allografts are not limited to the small amount of healthy donor tissue that can be safely harvested from an individual's joint. Also these allografts can be harvested from any region of the joint, allowing the surgeon to implant grafts taken from similar high load bearing areas[5]. With autologous chondrocyte implantation (ACI), chondrocytes are isolated from cartilage biopsies, expanded *in vitro* and seeded directly into the defect site[5,9].

In terms of clinical application of these resurfacing techniques, the origin of cartilage damage is an important consideration. With OA cartilage damage, ACI is not a suitable treatment option, while mosaic arthroplasty has yielded favorable results[15]. Also, as seen

with the previously mentioned repair strategies, inconsistencies between the reported findings of these methods are common[9,16,17]. Failure of these simple surgical interventions, or in severe cases of cartilage degeneration, total joint replacement may be the only treatment option[9,4].

With the exception of total joint replacement, complete restoration of joint function with other surgical techniques is highly contested in the literature[9]. One outcome that is shared between the different interventions is the high incidence of joint pain relief. However these favorable short-term outcomes have been shown to ultimately fail in long-term application[9].

## 1.3 Articular Cartilage Tissue Engineering

Successful reconstruction of articular cartilage should be characterized with both pain relief and complete restoration of joint function. As outlined in the previous section, there is no current treatment to adequately restore long-term joint function[18]. This absence, in conjunction with the poor regenerative capacity of articular cartilage has turned our focus towards regenerative strategies. Tissue engineering (TE) offers the promise of regenerating a tissue with the same structural and functional properties of native articular cartilage[19]. In general, articular cartilage is a prime candidate for tissue engineering because this tissue is avascular, aneural, and has a relatively simple composition[20].

Although there exists many different culturing methods employed in TE today, they have most frequently been developed in accordance to a three element model: i) cell source, ii) scaffold and iii) environmental factors.

Most culturing methods use a large amount of cells[1], requiring careful consideration of potential limitations associated with each cell type. For example, the chondrocyte concentration in cartilage is low, requiring either substantial tissue harvest or *in vitro* expansion of the cells[21]. While cell expansion is relatively easy, it encourages loss of the chondrogenic phenotype. However, chondrocyte dedifferentiation can be reversed; the seeding of expanded chondrocytes within a three-dimensional scaffold promotes the re-differentiation of these cells[20,22]. When culturing articular cartilage, it is important not to consider each culture element in isolation. As illustrated above with scaffold influence on chondrocyte behaviour, each element can have significant impacts on the culture system dynamics.

## 1.4 Remodeling of engineered constructs

### 1.4.1 *In vitro*

The literature of TE of articular cartilage has reported some success in the generation of hyaline-like tissue constructs. However, in comparison to native cartilage, these constructs are generally of inferior quality and durability[19]. Structurally, articular cartilage is organized vertically and horizontally throughout the tissue depth. This high

degree of architectural organization is a determinant factor in cartilage's ability to function in a mechanically demanding environment[1]. Initial attempts for cartilage engineering have resulted in the generation of a homogenous tissue[23]. Given the importance of structure in cartilage, the generation of a homogenous tissue may contribute to the compromised mechanical properties.

In an effort to achieve zonal organization similar to that of native tissue, *in vitro* culture should provide an environment that is conducive to articular cartilage growth. The addition of various biochemical and biomechanical signals into the culture system has been shown to encourage matrix remodeling, resulting in zonally stratified constructs[23,24]. Use of bioreactor systems not only generate highly reproducible environments, they also enable researchers to apply these signals (e.g. low-shear stress) in a controlled manner.

### 1.4.2 *In vivo*

The length of *in vitro* construct culture can influence its performance once implanted in the body. Studies have shown that longer culture periods can diminish a mature constructs capacity to integrate with surrounding articular cartilage[23]. In addition, as implantation of the construct within the joint is the ultimate end goal, it is important to consider the *in vivo* influence on remodeling of the construct. Constructs that are too old may not be able to integrate, but constructs that are too underdeveloped may not be suited to withstand the mechanical environment in the joint[23]. Animal models allow pre-clinical

evaluation of the engineered construct[23,25]. Although direct correlation between animal and human results is impossible, it is still important to establish clinical relevance with an appropriate model[25].

## 1.5 Research objectives

While current surgical interventions used for articular cartilage repair may offer temporary relief of symptoms, limited long-term applicability of these therapies is of concern. Common treatments rely on a large amount of donor tissue and/or further cell expansion that may elicit negative results. The purpose of this thesis was to characterize large-sized engineered constructs (3 $cm^2$) developed from a small population of cells and to assess their performance in a rabbit chondral defect model. The specific objectives of this thesis were to: i) determine optimal growing conditions for the constructs in a continuous bioreactor and ii) evaluate the reparative nature of the construct implanted in a rabbit defect model at three post-operative time intervals (1, 3 and 6 months).

In order to achieve the first objective, bioreactor parameters that were varied included sodium bicarbonate concentration (0, 15, 20, 25 and 30 mM) and culture time (2, 3 and 4 weeks). The use of a continuous flow bioreactor ensured adequate nutrient delivery to the developing constructs, while maintaining a low-shear environment. Resulting cartilaginous tissues were evaluated biochemically, morphologically and mechanically. Based on these results, constructs for implantation were grown at a 15 mM $NaHCO_3$ concentration for 3 weeks. The engineered tissue was then implanted in a rabbit model in

order to achieve the second objective. Upon euthanasia, rabbit knees were evaluated morphologically to assess the integration and survival of the implants. Histological, immunohistochemical and biochemical evaluation of the implants were performed to evaluate the repair capacity for up to 6 months post-operatively.

# Chapter 2

# Literature Review

## 2.1 Articular cartilage structure

Articular cartilage is the smooth hyaline tissue located in diarthrodial joints (i.e. knee, shoulder). With a tissue thickness ranging between 2 to 5 mm[26], it covers and protects the ends of two articulating bones (Figure 2-1). Synovial fluid, which acts as a nutrient source while also providing lubrication of the cartilage surface, enables almost frictionless coordination of the joint[1]. This unique connective tissue appears to have a relatively simple composition and is characterized by its aneural, alymphatic and avascular nature[27]. Due to its lack of blood vessels, articular cartilage relies primarily on nutrient diffusion from the synovial fluid for nutrition[28]. Unlike most tissues of the body, articular cartilage is not subject to typical wound healing responses, limiting its ability to heal itself upon injury. Cartilage is composed of an extensive extracellular matrix (ECM), which is created and maintained by one cell type: the chondrocyte[28].

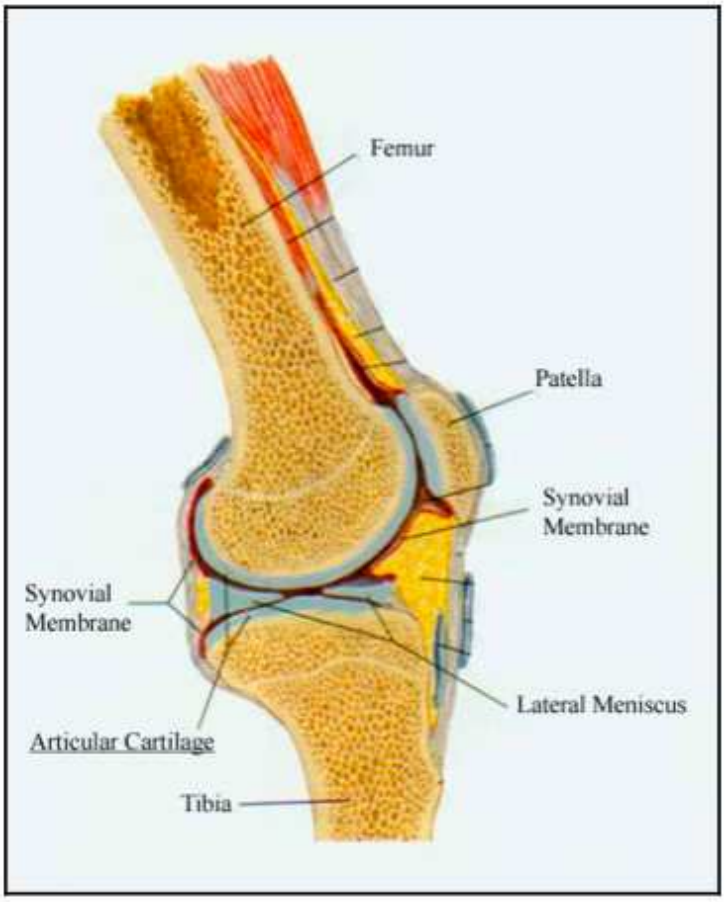


**Figure 2-1** Articulating surface of a human knee joint[29].

### 2.1.1 Chondrocytes

Articular cartilage is populated by one highly specialized cell type, known as the chondrocyte[3]. Although chondrocytes in adult cartilage account for only 1-2% of the tissue volume, they are solely responsible for cartilage tissue maintenance[1,27,30]. The role of the chondrocyte is to direct the metabolism of the ECM, including synthesis, degradation and maintenance. It is also responsible for the complex organization of these molecules within the ECM[3]. Due to its avascular nature, oxygen levels present in

cartilage can be as low as 1-3%. Unable to meet their energy requirements through aerobic respiration, chondrocytes rely primarily on glycolysis to generate enough energy for tissue maintenance[26].

The cells are not homogenously distributed throughout the tissue's thickness, with the highest cell density present at the surface of the tissue[26]. There appears to be little to no direct cell-to-cell communication between chondrocytes, but there are extensive cell-matrix interactions. Cell surface-binding proteins (e.g. integrins, CD44, etc.) allow the chondrocyte to receive various signals originating within the ECM[27]. These signals can be mechanical, electrical or physiochemical and will interact with the chondrocyte, allowing for regulation of its metabolic activity[26,27]. Chondrocytes maintain metabolic homeostasis with the secretion of collagen and non-collagenous proteins, as well as the enzymes that will degrade the ECM[12]. The cellularity in this tissue does not remain static throughout an individual's lifetime. With increasing age, there is a decline in cell content and a decrease in metabolic activity[27,32].

Within the three-dimensional ECM, chondrocytes generally possess a spherical morphology. When expanded in monolayer culture, the morphology is lost and usually accompanied with the loss of chondrogenic phenotype[33]. Loss of potency, as well as decreased ability to synthesize ECM macromolecules, are important considerations when culturing chondrocytes *in vitro*.

### 2.1.2 Extracellular matrix composition

The main constituents of the ECM are water, collagens and proteoglycans. A variety of other molecules are also present within the ECM but to a lesser extent. This matrix provides structure to cartilage, protection for the subchondral bone and also provides important signaling factors to the chondrocytes. The interactions between the fluid and solid phases of the ECM, impart the tissue with its extraordinary mechanical functions.

#### *2.1.2.1 Water*

The tissue's fluid is composed of water along with dissolved gases, electrolytes and metabolites[27]. Tissue water content will range between 65%, near the bottom of the tissue, to 80%, near the surface. Water flow across this tissue promotes nutrient transportation and aids in joint lubrication, while allowing the joint to withstand very high loads[28]. Water movement throughout the ECM requires large pressures due to the low permeability established by the protein network of the ECM. Tissue hydration and cation concentration of the fluid is largely dependent on the structural macromolecules in the ECM, particularly the negatively charged proteoglycans[3]. The other determinant of tissue hydration is the constraining force of the collagen network that serves to trap the 'hydrated' proteoglycans[28].

*2.1.2.2 Collagens*

Collagen is the main structural component of the extensive ECM. Although there are several types of collagen within articular cartilage, including type II, VI, IX, X and XI, all share a triple-helical structure[28,27]. The triple helix is a result of an association between three polypeptide chains. Each chain is composed of a characteristic three amino acid sequence repeat, in which glycine occupies the third position[28]. The other two positions can be occupied by any amino acid (other than glycine) but are most often occupied by proline or hydroxyproline. Hydroxylated amino acids allow the formation of covalent bonds that stabilize the collagen helix, as well as collagen fibril associations[28]. It is this collagen fibril network that has endowed articular cartilage with its unique tensile and shear properties[28]. Type II collagen represents over 90% of the total collagen and is distributed throughout the cartilaginous matrix. Both types IX and XI collagens associate with type II collagen, and it is these extensive cross-link networks that contribute to the insolubility of the cartilaginous matrix as well as its stability and strength[28]. Metabolism of the collagen network is relatively slow, when compared to other macromolecules in the ECM. The degradation of collagen in normal cartilage occurs at a slow rate. This process will accelerate with cartilage undergoing repair and remodeling (due to injury or skeletal growth) or degeneration[26,28].

*2.1.2.3 Proteoglycans*

Within the ECM, the interactions between the collagen matrix and proteoglycans are critical to the mechanical functions of articular cartilage[26]. Proteoglycans consist of a protein core covalently bound to glycosaminoglycan (GAG) chains. GAG chains are long, unbranched polysaccharides, containing multiple negatively charged carboxylate or sulfate groups[28]. These negatively charged groups repel one another, while also attracting cations in the water. This attraction is referred to as the Donnon osmotic pressure, facilitating interactions with water that can cause the tissue to swell[28]. There are three major types of GAG chains in cartilage including chondroitin sulfate, keratan sulfate and dermatan sulfate. Chondroitin sulfates are the predominant GAG in articular cartilage, ranging from 55 to 90% of the total GAG population. GAG composition and degree of sulfation can vary throughout the tissue and can change with an individual's age[28]. The presence of negatively charged groups can result in strong charge repulsive forces within the tissue and require the presence of cations in the water to help counteract this effect[28]. In articular cartilage, proteoglycans are generally found in large aggregating groups called aggrecans (Figure 2-2). The aggregan consists of a long protein core with varying amounts of chondroitin sulfate (up to 100 chains) and keratan sulfate (up to 50 chains), which are covalently bound to the core. Hyaluronan is an unbranched, unsulfated GAG, with which multiple aggrecan molecules will associate to form a large proteoglycan aggregate[28]. The N-terminal of the protein is where the aggrecan will bind to hyaluronan through its association with link protein. Although this bond is not covalent, this

interaction is stable and can be thought as irreversible without proteolytic degradation. Hyaluronan will also bind to the collagen network, anchoring the aggrecan within the ECM and preventing proteoglycan release during joint loading[27,3]. There are smaller proteoglycans, including decorin, biglycan and fibromodulin, present in cartilage and their role is mainly to stabilize the ECM[27].

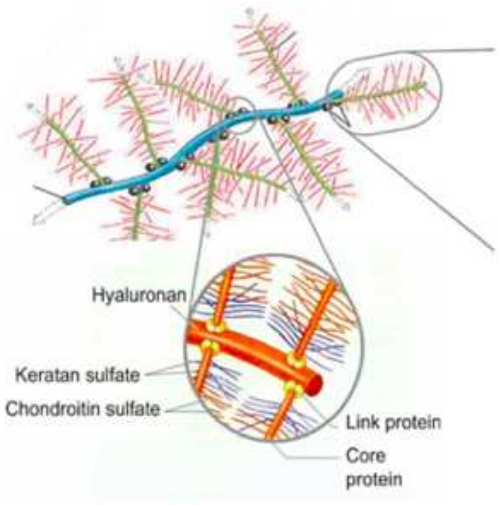


**Figure 2-2** Schematic representation of a proteoglycan aggregate[34].

### 2.1.3 Tissue organization

The highly organized articular cartilage can be divided into 4 zones: superficial zone, middle zone, deep zone and zone of calcified cartilage. The zones can be distinguished by one another according to their cell morphology along with ECM composition, organization and mechanical properties (Figure 2-3)[3].

The superficial zone is at the surface of the tissue, abutting on the synovial fluid. At 10-20% of the total tissue thickness, this zone may be the thinnest zone but it still possesses specialized mechanical properties[3]. The cells in this zone are relatively flat and are aligned parallel to the surface. The collagen network is also arranged parallel to the surface, oriented in the direction of load articulation[28]. The fibrillar orientation is a determinant factor in the mechanical properties of this tissue, providing it with tensile stiffness and strength[3]. The lack of sulphated proteoglycans, such as aggrecan, and highest percentage of water content, are other distinguishing features of this zone. The next zone down is the largest zonal division and is called the middle zone. The cells in this zone have a more rounded appearance but are present in lower concentrations. With increasing tissue depth there is an increase in collagen fibril diameter and proteoglycan concentration. In comparison with the superficial zone, lower collagen and water levels are present and the collagen network appears less organized at this zone. The deep zone is underneath the middle zone and is characterized by low cell content, large collagen fibril diameter and high proteoglycan levels. The chondrocytes in this zone are spheroidal and align themselves in a columnar fashion, perpendicular to the joint surface. This perpendicular arrangement is also reflected in the collagen fibril orientation. The deepest zone is the calcified cartilage zone. The tidemark separates the uncalcified cartilage from the subchondral bone below[1,28].

There is also regional organization in the ECM around each chondrocyte, which is divided into three regions depending on the chondrocyte's proximity to the ECM (Figure 2-3). The first two regions (pericellular and territorial regions) have regulatory influence on the chondrocyte[35]. The pericellular region is the location for cell attachment to the ECM and is rich in proteoglycan content, along with other non-collagenous proteins. The pericellular region is surrounded by the territorial region. The presence of thin collagen fibril assembly in this region may serve to protect chondrocytes when mechanical stresses are applied to the tissue. Increases in collagen fibril diameter indicate the beginning of the third region, the interterritorial region. Orientation of the collagen fibrils is dependent on their zonal location. This is the largest region of the tissue and endows the tissue with most of its mechanical properties[3,28].

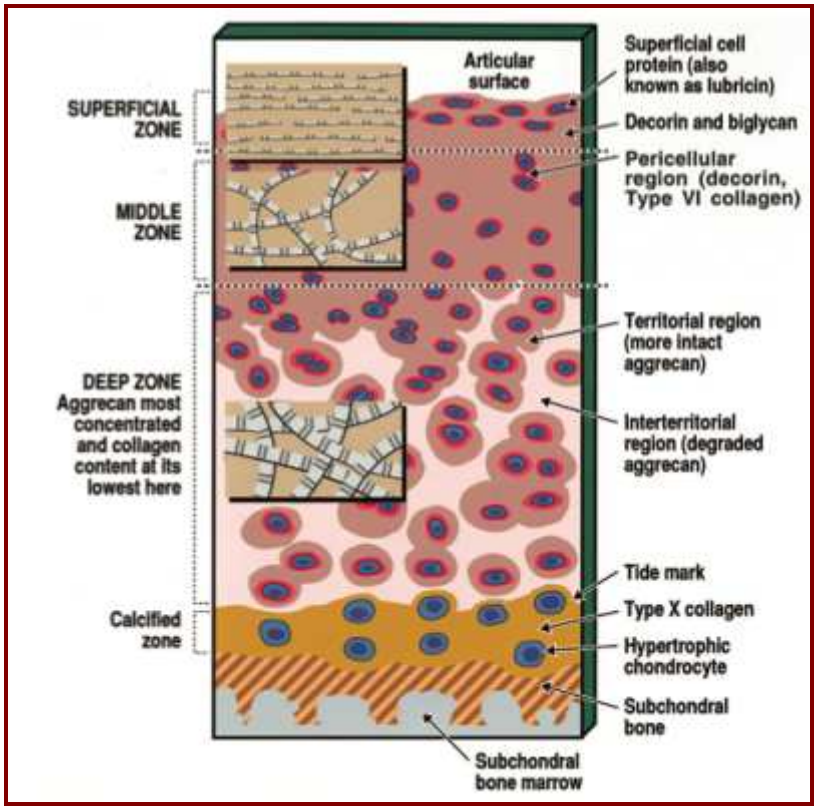


**Figure 2-3 An illustration of the zonal and regional organization of articular cartilage** [1]

## 2.2 Cartilage biomechanics

Throughout an individual's lifetime, articular cartilage is subjected to high loads that can be static, cyclical and/or repetitive. These loads must be efficiently distributed and transmitted across the joint surface to the subchondral bone to prevent wear and structural damage[23,28,]. To understand the mechanical properties of articular cartilage, it is useful to describe the tissue as a biphasic, viscoelastic material[28].

### 2.2.1 Biphasic nature

Articular cartilage is composed of two phases: a solid phase (protein/polysaccharide matrix) and a fluid phase (water and dissolved ions)[28]. The structural molecules of the matrix, including collagen and proteoglycans, are organized into a solid 3D matrix that is both porous and permeable. Water is retained within these microscopic pores until a pressure gradient or compression is applied to the matrix. In response to the application of a pressure gradient, water and ions will flow through the matrix. This fluid flow, will in turn, result in a large frictional drag on the solid matrix, inversely proportional to the permeability of the tissue[36]. Fluid pressure can support significant loads, reducing the stress on the solid matrix and is the major mechanism of load support within a joint[28,36].

### 2.2.2 Viscoelasticity

Articular cartilage is also a viscoelastic material; in response to a constant load or deformation, cartilage will exhibit a time-dependent behavior[28]. A viscoelastic material will respond to constant loading and constant deformation with creep and stress relaxation, respectively. The creep response is a time-dependent increase in deformation under constant load, until equilibrium is reached. The stress-relaxation response, on the other hand, is a time-dependent drop in stress under constant deformation, until equilibrium is reached[28]. Cartilage's viscoelasticity behavior can be attributed to two mechanisms: 1) flow-independent and 2) flow-dependent. Intermolecular friction of the solid matrix, including electrostatic interactions between collagen and proteoglycans,

causes the flow-independent mechanism. Fluid flow and frictional drag of the fluid phase are responsible for the flow-dependent viscoelasticity of cartilage[28,36].

## 2.3 Surgical repair strategies for articular cartilage

Although articular cartilage is designed for longevity, it can fail by injury and/or disease. Damaged cartilage is rarely returned to its original state by natural processes and will often require clinical intervention for pain relief and restoration of function[37]. Currently there is an absence of medications that promote healing of articular cartilage defects[38]. Thus, therapeutic interventions for the treatment of damaged articular cartilage are surgical and fall under three categories. The first are techniques whose main goal is to provide pain relief, rather than restoration of joint function. Lavage and debridement are two examples of this type of therapy. Whereas lavage involves rinsing of the joint surface with a solution, debridement combines lavage, in conjunction with excision of damaged /diseased cartilage[9]. The second type are techniques that promote the natural healing capacity of cartilage, including abrasion athroplasty, drilling or microfracture[39]. The final category includes techniques that involve resurfacing of cartilage, in which defects can be filled with cells (autologous chondrocyte implantation) or grafts (mosaicplasty)[38,39].

### 2.3.1 Defect classification

Articular cartilage defects can be divided into two categories, depending on the defect depth: 1) chondral defects and 2) osteochondral defects. Chondral defects can be partial-thickness (defect contained entirely within the cartilage) or full-thickness (defect extends down to the bone)[40]. Purely chondral defects do not penetrate the underlying subchondral bone, preventing the recruitment of pluripotent progenitor cells from the bone marrow[8]. Spontaneous repair is not seen with chondral defects, as the chondrocytes near the injury are unable to fill in the defect with repair tissue. However, in some circumstances 'matrix flow' will occur, resulting in the migration of adjacent ECM towards the empty defect surface. Conversely, osteochondral defects penetrate the subchondral bone, exposing the defect area to mesenchymal stem cells and growth factors. Typically with this repair response, blood will fill the defect, along with mesechymal stem cells resulting in the formation of fibrocartilage (a fibrous type of cartilage). The properties of the newly formed tissue are inferior to those of native cartilage, both structurally and mechanically, and the fibrocartilage does not integrate well with surrounding native cartilage[8,9]. Repair of these defects is usually short-lived and will eventually be followed by degeneration of the fibrous tissue, as well as the adjacent native cartilage[8]. The incidence of spontaneous repair response is also limited to a critical size, involving only those defects that fall within the narrow size range[9].

### 2.3.2 Techniques promoting natural repair

Spontaneous repair, observed in osteochondral defects, is the rationale behind bone marrow stimulation techniques, including abrasion arthroplasty, pridie drilling and microfracture[9,5]. Cartilage degeneration is treated surgically by penetrating the underlying bone-marrow spaces, thereby releasing progenitor cells into the defect area. However success rates of these techniques tend to be highly variable, non-reproducible and patient-specific (age, activity level and various other factors influence the repair outcome)[9]. Filling of the defect ranges from no tissue, to fibrocartilage, to hyaline-like cartilage or a mixture of both. Even in the absence of long-term joint function restoration, these techniques have been shown to offer patients substantial relief of joint pain[9].

Microfracturing is still the most commonly employed method as a first-line treatment of damaged cartilage. Studies have reported positive outcomes for this technique that continue for up to 5-7 years[9,41,42]. Unlike other resurfacing techniques, these strategies require a single surgical intervention and do not require the need to harvest healthy donor tissue.

### 2.3.3 Cartilage resurfacing techniques

The repair tissue from bone marrow stimulating techniques is ill equipped to withstand the mechanically demanding environment of the joint. As a result it will eventually breakdown and ultimately fail in its repair of defects. The main goal of cartilage

resurfacing techniques is to increase the durability of the repair tissue, allowing for long-term restoration of joint function and pain-relief. These strategies do not rely on articular cartilage's poor intrinsic repair capacity, but rather the defect regions will be filled with hyaline or hyaline-like cartilage. Autologous chondrocyte implantation (ACI) and mosaicplasty are the two most commonly used resurfacing techniques.

*2.3.3.1 Autologous chondrocyte implantation*

Autologous chondrocyte implantation (ACI) was initially described by Brittberg *et al.* in 1994 and is characterized by three separate stages[43]. At the first stage, a small cartilage biopsy is harvested arthroscopically from a low-weight bearing area of the joint. Once excised, the tissue is digested enzymatically and the isolated chondrocytes are expanded in culture for 2-3 weeks. The initial number of required chondrocytes varies between studies, with expansion of the harvested chondrocyte ranging from twenty to fifty times their initial concentration[144]. The final step involves a second surgical procedure in which the cultured chondrocytes are injected beneath a periosteal patch sutured over the defect site[43,44]. Current clinical applications of ACI procedures implant cells at a density of 30 x $10^6$ cell/mL[144]. The periosteal patch acts like a barrier, trapping the chondrocytes in the defect area, where they can initiate ECM production. Encouraging results, including pain reduction and restored joint function have been demonstrated in a number of clinical studies[13,44,45]. Brittberg *et al*.[13] reported good-to-excellent results in 60-90% of the treated patients, with 90% success rate for femoral condylar defects. Long-term evaluation of

this procedure in one study found that successful outcomes with this treatment could last for as long as 11 years[46].

Histological analysis of the repair tissue in one study revealed that ACI is capable of producing a hyaline-like tissue in some specimens[42,47,48]. But it is important to note that none of these samples were morphologically or histochemically identical to hyaline cartilage and can at best be labeled fibrocartilage. The formation of fibrocartilage in the defect region, in place of hyaline cartilage, has been confirmed by other investigators[9]. Other studies, including Breinan *et al*.[16], reported no significant differences in the repair response between treated and control defects in their canine model. The large discrepancy in results between studies is confounded by the fact that the origin of the repair tissue is still unknown. Critics of the ACI procedure maintain that chondrocytes expanded *in vitro* will undergo dedifferentiation in monolayer culture and the dedifferentiated cells would not support the formation of a hyaline-like tissue and likely some other factor contributed to the repair response[9].

In addition to conflicting findings, there is no clinical data that suggests ACI is more effective in treating cartilage defects than other therapeutic strategies[49]. In conjunction with a high cost, to the need for two surgical interventions and cell culture, ACI is at a disadvantage in comparison to other treatment protocols.

*2.3.3.2 Mosaic arthroplasty*

Mosaic arthroplasty, also known as osteochondral transplantation, is a technique that can be used in the treatment of both chondral and osteochondral defects. It was developed around the same time as ACI[50,51] and involves the filling of a defect with autologous osteochondral plugs. Cylindrical plugs are harvested from low-weight bearing regions of the joint and placed in the defect, creating a 'mosaic' pattern[42]. These osteochondral plugs are cut in varying sizes, allowing for maximal filling of the defect. The small gaps remaining between plugs will eventually be filled with fibrocartilage. Clinical application of this procedure in human patients has resulted in positive short-term results in both pain relief and improved joint functionality (good to excellent results in 60-90% of cases)[9,52,53]. To date, Hangody *et al*.[14] have published the largest series of mosaic arthroplasty procedures, including 597 femoral condylar defects and 118 patellar defects. Outcomes were followed up to 10 years after surgeries, with successful results in 92% of condylar defects and 79% of patellar defects.

In comparison to ACI, randomized clinical trials have found no significant difference in repair outcomes for both treatments[17,54]. In terms of recovery time, patients treated with mosaic arthroplasty recovered faster than with ACI. Also it should be noted that the osteochondral transplants retained their hyaline character throughout short-term evaluation, while ACI repair tissue consisted of mainly hyaline-like cartilage[17].

As with any existing cartilage repair strategy, there are several limitations associated with mosaic arthroplasty. One issue is with donor site morbidity. In order to fill a defect, healthy tissue must be excised from normal sites of a joint, thus creating another defect[9]. But rather than cause further joint degeneration, the small defects are subject to spontaneous repair and are usually filled with a fibrous tissue. It is rare that these donor sites would have an adverse effect on joint function[55]. Ideal defect sizes for this treatment are small to medium (between 1 and 4 $cm^2$), with availability of donor tissue as the main factor limiting defect size[52]. Another consideration for this procedure is potential graft failure and degeneration of surrounding native cartilage. Chondrocyte death at the periphery of the graft is inevitable with current tissue harvesting methods. Few studies have looked into the extent of viability in osteochondral grafts and its impact on adjacent native cartilage[9,43]. Diminished chondrocyte viability at the edge of the graft may also contribute to poor lateral integration with surrounding cartilage. The absence of lateral support can lead to rapid degeneration of both graft and native cartilage[9].

### 2.3.4 Tissue Engineering

An effective treatment is one that produces results that are reliable and durable. Current articular cartilage repair procedures have yet to satisfy these requirements. All of these procedures have limitations and have been unable to reproduce repair tissue that is biochemically and mechanically identical to that of hyaline cartilage. Recent focus has turned towards tissue engineering, with the potential to provide permanent solutions to

cartilage damage. Tissue engineering is an evolving field that relies on a three-element model (the tissue engineering triad): cell source, scaffolds, and environmental factors (growth factors, bioreactors, mechanical stimuli)[6].

*2.3.4.1 Cell Source*

There are multiple potential cell types to consider for use in cartilage tissue engineering. Each type has its advantages and disadvantages. Primary and chondrogenic cell lines seem to be the intuitive choice, but they are often present in low concentrations and expansion can lead to dedifferentiation of the cells. Mesenchymal stem cells can be obtained from bone marrow and are present in larger concentrations. These cells are capable of multi-lineage differentiation including the chondrogenic lineage[56]. In comparison to chondrocytes, cell expansion can be performed on the mesenchymal stem cells with little effect on the quality of tissue formed *in vitro*[5]. In addition, these cells have also been shown their ability to differentiate into bone cells, demonstrating their utility with osteochondral tissue cultures[5].Another source is embryonic stem cells, with studies having demonstrated the chondrocyte differentiation potential of these cells. However, ethical concerns and safety issues have limited the widespread use of this embryo-derived cell source[56]. The potential for chondrogenic lineage is not limited to stem cells and studies have shown this ability in periosteal cells[9]. These cells have been shown to positively influence articular cartilage's healing response with implantation.

However, the survival of these cells within the repair tissue appears to be short-lived, limiting the long-term capacity of the repair tissue[9].

Autologous chondrocytes for tissue engineering have the added benefit of their extensive application in clinically approved procedures for cartilage repair (i.e. ACI). Filling a clinically relevant defect requires a substantial of cell population[57]. As only a limited amount of cells can safely be harvested from a patient, chondrocyte proliferation can be accomplished using monolayer culture. Chondrocyte dedifferentiation tends to occur with monolayer expansion, decreasing the chondrocyte's ability to synthesize proteoglycans and type II collagen[57]. The loss of chondrogenic phenotype is reversible and can be re-expressed once the cell is placed in a suitable 3D structure[33,58,59].

The use of chondrocytes from allogenic tissue allows researchers to bypass the limitations associated with autologous chondrocytes. An important consideration when using allogenic cells is potential immunogenic reactions that can result in graft resorption or rejection. Lacking vasculature, articular cartilage has been described by many as immunoprivileged[25]. Although chondrocytes contain antigens that could elicit an immune response, studies have found immunogenic reactions are negligible when they are contained in a matrix. This is likely due to the protective barrier provided by the matrix of tissue grafts and engineered constructs, isolating the chondrocytes from the host's immune system[25].

*2.3.4.2 Scaffolds*

Stripped to its minimal function, a scaffold suitable for tissue engineering purposes facilitates cell retention and accumulation of ECM. Also, depending on the geometry of the defect, it must also be able to accommodate various shapes and sizes[33]. Scaffolds serve to repopulate a defect area with cells in two different ways: delivery or induction of cells. Cells can be seeded on the scaffold pre-implantation or a cell-free scaffold can be implanted allowing neighboring cells to migrate[5,60].

A number of scaffold materials have been investigated for cartilage tissue engineering and they are typically made from natural or synthetic polymers. There are many factors to consider when choosing a scaffold material, including but not limited to biocompatibility, biodegradability, mechanical properties, surface chemistry and sterilizability[33]. In general the use of natural polymers (collagen, hyaluronic acid, fribrin glue) has the advantage of fewer biocompatibility issues. However, clinical application of these matrices may be limited due to low supplies of these materials, as well as potential issues arising from antigenicity and disease transfer[9]. While synthetic polymers (polyglycolic acid, poly L-lactic acid, polyurethane) may not be limited by their supply, biocompatibility and biodegradation issues with these materials can have undesired effects on the repair process[9, 40].

Once the scaffold material is chosen, it must be sufficiently mechanically resilient to withstand the harsh environment in the joint. Ideally, the material will also degrade at the same rate as ECM deposition, allowing itself to be replaced by newly synthesized cartilage. Similarly, the by-products released during scaffold degradation should not induce inflammatory and immunogenic responses, to avoid negative impacts on the repair process[33]. Despite the variety of materials and advances in scaffold development, mechanical properties and biochemical composition of the engineered constructs are still inferior when compared to articular cartilage's ECM[59] .

The three-dimensional structure provided by a scaffold is essential for the conservation of chondrocytic phenotype. Although it would seem that scaffolds are necessary for cartilage regeneration, there are some researchers who have developed a scaffold-free approach to chondrocyte culture[61]. During embryonic cartilage development, cartilage synthesis is facilitated by the condensation of cells[57]. Studies have found that higher initial cell seeding densities within the scaffold allows for increased ECM synthesis and deposition[57,62]. Alternatively, other attempts to mimic the natural condensation of the cells have been employed in scaffold-free cultures. Isolated chondrocytes centrifuged to form a pellet, allowing for close cellular interactions to stimulate chondrogenesis while avoiding cellular dedifferentiation[50,51,52]. Studies maintain that pellet cultures support a chondrocyte phenotype, and yield a cartilaginous tissue rich in type II collagen.

### 2.3.5 Bioreactors for cartilage tissue engineering

The introduction of bioreactors as a culturing tool is ideal for tissue engineering as they enable large-scale application of these techniques. Bioreactors can provide an environment that is highly reproducible, controllable and can enable the automation of the processing steps[65]. Although the main goal of tissue engineering is successful generation of a biological model, it is also important that these culture strategies are both efficient and economic in their application[66].

The generation of 3D tissues is limited to the supply of oxygen and metabolic nutrients. If the engineered constructs are to be used for tissue replacement, they will need to be a significant size. Diffusion of nutrients becomes a limiting factor when tissue diameter exceeds 100-200 μm[67]. To bypass this limitation, researchers look towards bioreactors that increase the rate of mass transport[65]. Another benefit of using bioreactors is associated with the unique *in vivo* mechanical environment. The mechanical stresses encountered in the joint play a central role in metabolic events within the ECM[68]. One role of the bioreactor is also to provide a controllable environment that mimics that of the body. A bioreactor can be as simple as a Petri dish or a dynamic system providing physical cues to the growing construct. Thus, the aim of the modern bioreactor is twofold: to increase of mass transfer to the growing tissue and provide mechanical stimulation during tissue growth[56]. There are various types of bioreactors that accomplish

these two goals, including mechanically stirred bioreactors, low shear bioreactors and perfusion bioreactors.

*2.3.5.1 Mechanically stirred bioreactors*

The spinner flask is a common example of this type of bioreactor (Figure 2-4)[67]. This is a simple system in which cell-seeded scaffolds are suspended in the reservoir and continuous media mixing is achieved by the use of a magnetic stir bar. High stirring velocities can be used (e,g, 50 rpm) to overcome the diffusion limit but results in a mechanical environment characterized by high-shear stresses, produced by turbulent eddies originating in the reservoir [67]. Cell damage typically does not occur at these velocities, but the high shear stresses are not conducive to cartilaginous tissue growth and a fibrous protective shell can form around the constructs. With these mixed cultures, collagen content has been shown to increase between 50 to 125%[69,70]. These results may be misleading if a fibrous shell is formed which is composed primarily of type I collagen. Although this method is typically not optimal for articular cartilage growth, it has another important application in tissue engineering. These mechanically stirred bioreactors enable efficient cell seeding of scaffold, superior to that of static seeding. When seeding the scaffolds, the mixing in this system not only results in a homogenous distribution of cells but also better scaffold attachment and overall ECM formation[71].

*2.3.5.2 Low shear bioreactors*

The rotating wall vessel (RWV) bioreactor also provides increased mass transport but does so in a low shear environment (Figure 2-4). The RWV is a hydrodynamic bioreactor that was originally designed by NASA to mimic microgravity[5]. The inner cylinder remains stationary and is also the location for gas exchange with the external environment. The outside cylinder can be rotated at a speed that allows the construct to remain in a state of free-fall. Due to the relatively low rotating speeds, the constructs are typically in a laminar flow stream[65] and the negative influence of turbulent eddies is generally not a concern. In this reactor, there are three forces that act on the constructs: centrifugal force, gravitational force and drag force[67]. In comparison to static or mixed cultures, RWV culture of cartilaginous constructs results in large increases in proteoglycan and type II collagen content. Pei *et al*.[72] found that the mechanically environment induced in a rotating bioreactor produced larger cartilage-like constructs that had superior structural, functional and mechanical properties.

*2.3.5.3 Perfusion Bioreactors*

Perfusion bioreactors involve the continuous flow of medium through, or around, the construct (Figure 2-4). A peristaltic pump is typically used to provide medium flow. This eliminates the need to manual change the medium, resulting in a decreased risk of contamination[71]. The fluid flow across the construct results in mechanical stimulation in

the form of shear stresses. The magnitude of the applied shear stress is dependent on the flow rate of the system[67].

In 2000, Pazzano *et al*.[73] used a perfusion bioreactor for the growth of cartilaginous constructs, which had superior ECM composition when compared to static cultures. Other studies that have employed perfusion bioreactors with chondrocytes have indicated increases in type II collagen, as well as the absence of type I collagen. However the percentage of collagen type II was still markedly lower than that of native cartilage[74]. Another concern is finding the optimal fluid flow rate. High flows rates are associated with high shear stresses, while low flow rates can result in inconsistent tissue growth throughout the scaffold thickness. This result highlights the need to establish a balance between the rate of mass transfer and the level of shear force on the construct[71].

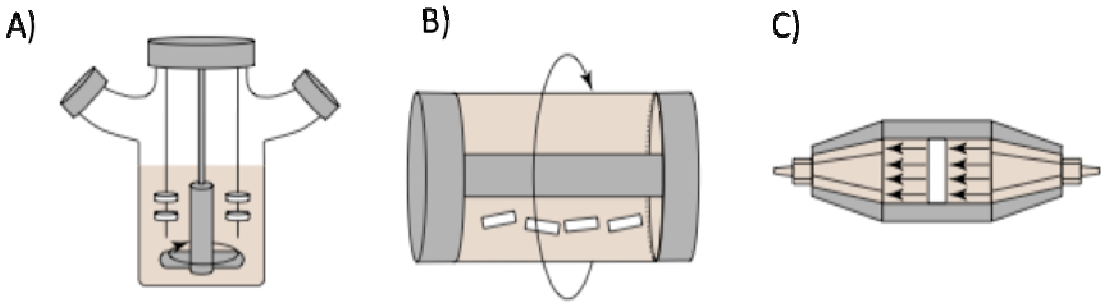


**Figure 2-4** Schematic representation of current bioreactors. A) Spinner-flask bioreactor B) Rotating-wall vessel and C) Direct perfusion bioreactor[65]

### 2.3.6 Animal models for cartilage repair

The ultimate goal for tissue-engineered constructs would be to regenerate hyaline cartilage structurally and functionally identical to its native form. Evaluation of the biochemical and mechanical properties of *in vitro* constructs is crucial to characterize their hyaline-like nature. Currently there are no standard evaluation methods to assess these parameters. In general, positive indicators for articular cartilage development include the production of type II collagen and sulfated proteoglycans, as well as the absence of type I collagen production[71]. However, successful joint function restoration does not necessarily require repair tissue to be identical to hyaline cartilage. It does require that the repair tissue is functionally equivalent to that native cartilage. As a result, there has been a shift in the focus towards characterization of the functional nature of the repair tissue[40]. *In vitro* studies can provide valuable information on the development of the cartilage constructs but cannot provide a prediction of construct functionally after implantation. The logical next step would involve the *in vivo* performance of the construct in an appropriate animal model.

As experimental animal joints are physiologically and anatomically different from human joints, direct application of these models to a clinical setting can be challenging[40]. However, there are many variables in an animal model that can be tailored to address the *in vivo* repair potential of engineered constructs.

In terms of anatomical applicability of experimental animals, the mechanics of the joint must be considered. In the human knee joint, articular cartilage has a compressive modulus ranging from 0.5 - 1.8 MPa[75,76,77]. The modulus will be influenced by a number of factors, including: location within the joint, biochemical composition. In low-weight bearing areas, such as the patellar groove, the modulus will be at its lowest value (~0.53 MPa)[77]. This trend has also been observed in other species (e.g. bovine, dog, rabbit and monkey). The rabbit knee exhibits morphological similarities with the human knee joint, and as such the rabbit model is well documented in cartilage research[78]. Even though larger animals (dogs, goats, horse) have been found to more closely resemble human joints in comparison to smaller animals (such as rabbits), their selection may not be practical in terms of expenses and housing[40,78]. Once an appropriate animal species has been chosen, variables including animal age, type and location of defect and implant fixation must be considered.

*2.3.6.1 Animal age*

Animal age will influence cartilage's potential for repair. Superior wound healing of articular cartilage has been demonstrated with immature animals[40], leading initial investigations of engineered constructs to be performed in younger animals. Successful outcomes should be repeated in skeletally mature animals, as most patients requiring cartilage treatment are adults. The age of harvested chondrocytes is another important consideration for repair. Older chondrocytes have shown decreased proliferation,

metabolism and production of ECM[79]. Rejuvenation of older chondrocytes is of great interest and studies have shown its potential with cell culture[79,80].

*2.3.6.2 Location and type of defect*

Defects created in animal models can vary in size, location (patellar groove vs. femoral condyle) and type (osteochondral vs. chondral) and each of these parameters can influence the repair potential of the construct. Spontaneous repair can occur in small-sized osteochondral defects. The maximum size at which spontaneous repair can occur is termed the "critical defect size" and can vary between animals[40]. The location of the defect will determine the mechanical environment. Engineered constructs that survive and encourage repair in the patellar groove may not perform as well in high-weight bearing regions, such as the femoral condyles.

*2.3.6.3 Implant fixation*

Without formal fixation of the construct within the defect, loss of the engineered construct is a concern, especially when dealing with purely chondral defects[81]. Common methods of construct fixation include press fitting, sutures, fibrin glue or a mixture of all three[40]. Osteochondral implants are generally secured using press-fit alone, as to minimize interactions with defect repair that can arise with additional fixation. Mainil-Varlet *et al*.[82] examined construct retention rate using press-fit fixation with chondral and osteochondral defects. With a defect diameter of 4 mm and corresponding cartilage

implant of 4.1mm diameter, the constructs were press-fitted into the defect. Implant loosening was observed in 55% of chondral defects and only 8% of full-thickness defects. As construct loss is to be expected with chondral defects, a combination of fixation techniques is often used.

# Chapter 3

# Development of Large-Sized Engineered Cartilage Constructs without a Separate Cell Expansion Phase

## 3.1 Abstract

Confronted with articular cartilage's limited capacity for self-repair, joint resurfacing techniques offer an attractive treatment for damaged or diseased cartilage. While current tissue engineering approaches have been able to generate cartilage-like constructs, they require a substantial amount of cells and/or a separate cell expansion phase to generate sufficient quantities of implantable tissue. As routine cell expansion methods tend to elicit negative effects on cell function, this study describes an approach to generate phenotypically-stable, large-sized engineered constructs ($\geq 3$ $cm^2$) directly from a small number of isolated young rabbit chondrocytes (approximately 20,000 per construct), without the use of a scaffold. The bioreactor cultivated constructs are hyaline-like in appearance and possess an immunohistochemical composition similar to that of native articular cartilage. The effect of different seeding methods and culture time on the biochemical and mechanical properties of the developed constructs was examined, as well as the efficacy of cartilage repair in an animal defect model. After implantation, the constructs experienced further remodeling approaching the properties and zonal organization of the native tissue. Additionally, the possibility of generating constructs

matched to the shape and surface geometry of the patient's anatomy through the use of rapid-prototyped defect molds was explored.

## 3.2 Introduction

Osteoarthritis currently affects around 27 million Americans; a conservative estimate that will continue to rise with a progressively aging population[26]. This disease is characterized by a breakdown of articular cartilage resulting in pain and possible loss of joint function. Currently there is an absence of long-term repair strategies for diseased or damaged articular cartilage and conventional approaches tend to be more palliative in nature[80]. The need for new repair strategies, in conjunction with the limited capacity of cartilage self-repair, has turned the focus towards regenerative medicine. Joint resurfacing with a tissue formed *in vitro* is a promising new approach for cartilage repair, but has yet to be realized clinically. Isolated cartilage cells (chondrocytes) grown in three-dimensional culture have been shown to maintain their phenotype, enabling the synthesis of a cartilaginous extracellular matrix (ECM) similar to that of native tissue[83]. Although much progress has been made in refining this approach, it has still proven challenging to produce sufficient quantities of tissue suitable for the repair of clinically-sized cartilage defects (1.5 – 6.5 $cm^2$)[13].

The number of cells that can be reasonably extracted from a single individual is restricted (~ 180,000 – 455,000 cells per 300 – 500 mg biopsy), as the extraction of autologous tissue can place a significant stress on the donor sites[13]. The common approach to address this problem has been to include a cell expansion phase before seeding the cells in, or on, a suitable scaffolding material[33]. Using this approach, the resultant engineered constructs

tend to become hyper-cellularized[84,85,24,79] which can be further exacerbated as routine cell expansion methods also tend to elicit negative side effects such as de-differentiation and loss of potency[20,22,86]; thus requiring a vast number of cells to synthesize sufficient quantities of tissue. Although the re-differentiation of serial passaged cells can be achieved by various means (e.g. growth factor stimulation, encapsulation)[22,87,88], aged chondrocytes (those which would typically be used clinically) tend to lose their sensitivity to most chemical and environmental stimuli[80,89] thus limiting the effectiveness of this approach.

Here a novel approach is described in which phenotypically-stable, large-sized tissue engineered cartilage constructs ($\geq 3$ cm$^2$) are developed directly from a small number of isolated cells (approximately 20,000 per construct), without the use of a cell expansion phase. The scaffold-free engineered cartilage constructs are developed within a continuous flow bioreactor[90,91] that results in extensive growth of neo-tissue that conforms to the size and shape of the reactor vessel. Tissue growth is simulated by the continuous flow of culture media as these anaerobic cells rapidly deplete nutrients from the media[92,93]. In addition, the media is supplemented with bicarbonate to provide neutral pH within the reactor to further stimulate the synthesis of cartilaginous extracellular matrix (ECM) macromolecules[91,94,95,96] and ensure phenotypic stability of the developed constructs. To test the versatility of this approach, the effect of three different seeding methods and culture time on the biomechanical properties of the developed constructs

was examined. Once the parameters were optimized, assessment of the construct's efficacy to repair critical-sized defects in a rabbit model was performed. Lastly, the possibility of generating constructs matched to the shape and surface geometry of the patient's anatomy was explored through the use of rapid-prototyped defect molds.

## 3.3 Materials and Methods

### 3.3.1 Rabbit chondrocyte harvest and isolation.

This study was performed with approval from the University Animal Care Committee (UACC) at Queen's University. Full thickness articular cartilage slices were harvested from the femoral condyles of young female New Zealand white rabbits (2 $\pm$ 0.5 kg) (Charles River, Wilmington, MA). Animals were sedated with acepromazine (1 mg/kg intramuscular injection) followed by a lethal overdose of sodium pentobarbital (100 mg/kg). Immediately after euthanasia, the hind legs were removed from the torso and dissected aseptically within a UV sterilized laminar flow hood on the same day that the rabbits were sacrificed. The cartilage slices were digested with 0.5% protease (w/v) (Sigma-Aldrich, Oakville, ON) followed by 0.15% collagenase A (w/v) (Roche Diagnostics Canada, Laval, QC) in Ham's F12 media (Hyclone, Logan, UT, USA) supplemented with 25 mM HEPES (4-2(2-hydroxyethyl)piperazine-1-ethanesulfonic acid) (Sigma-Aldrich) and an antibiotic solution containing: 100 U/mL penicillin, 100 μg/mL streptomycin and 0.25 μg/mL amphotericin B (Sigma-Aldrich)[97] overnight at 37°C with 95% relative humidity and 5% $CO_2$. After incubation, the digest was passed through a 200 mesh filter (Sigma-Aldrich) to remove any undigested tissue and bone fragments. Chondrocytes were isolated by centrifugation (600 x g for 7 minutes) and the resultant cell pellet was washed 3 times with Ham's F12 media. Cell viability was determined by Trypan Blue dye (Sigma-Aldrich) exclusion[98].

### 3.3.2 Agarose chondrocyte culture and determination of optimal sodium bicarbonate concentration.

Isolated chondrocytes were seeded in 2% (w/v) low-melting point agarose gels (type VII, Sigma-Aldrich) in phosphate buffered saline (PBS, pH 7.4) at a final cell concentration of 5 x $10^5$cells/mL and then cast in 50 μL molds for 30 min at room temperature. Cell seeded agarose disks were cultured in 24-well culture plates with 1 mL of Ham's F12 medium supplemented with 20% FBS (v/v) (Sigma-Aldrich), 1X antibiotics and 100 μg/mL ascorbic acid (Sigma-Aldrich) and varying concentrations of sodium bicarbonate ($NaHCO_3$, Sigma-Aldrich) (0, 15, 20, 25 or 30 mM). The upper bound of 30 mM was chosen as higher concentrations of $NaHCO_3$ resulted in media pH greater than 7.5[94]. Cultures were grown for two weeks at 37°C with 95% relative humidity and 5% $CO_2$ with media changes every 2-3 days.

To determine the optimal $NaHCO_3$ concentration for bioreactor culture, ECM synthesis was determined by radioisotope incorporation. Prior to final media exchange, cultures were incubated in the presence of [$^{35}$S] sulphate and [$^{3}$H] proline (5 μCi of each isotope, PerkinElmer, Waltham, MA, USA), to label newly synthesized proteoglycans and collagen, respectively[99,100]. After 24 hours of incubation, cell seeded agarose disks were washed in PBS (pH 7.4) and each disk was digested in papain (40 μg/mL in 20 mM ammonium acetate, 1mM ethyldiaminetetraaceetic acid (EDTA) and 2 mM dithiothreitol (DTT), Sigma-Aldrich). One hundred microlitres aliquots were taken from each digested

sample and radioisotope incorporation was then measured using a β-liquid scintillation counter (Beckman Coulter, Mississauga, ON) and normalized to the DNA content of culture using the Hoechst 33258 dye assay[101].

### 3.3.3 Continuous flow bioreactor.

A continuous flow bioreactor system was used to maintain a constant medium supply to the developing constructs in a low-shear environment[90,91]. Briefly, the reactor consisted of multichannel vented polypropylene chambers to house single constructs (3 $cm^2$ containing a maximum media volume of 3.93 mL) (Figure 3-1). Each chamber had an inlet port at the base of the well and an outlet port at the top, preventing the accumulation of waste products within the chamber. A constant flow of fresh media (from aerated reservoirs) at 10 μL/min was provided by a peristaltic pump (Ismatec, Cole Parmer Canada, Anjou, QC) with waste media collected in a vented reservoir. The bioreactor was housed in an incubator maintained at 37°C with 95% relative humidity and 5% $CO_2$ (Appendix A, Figure A 1).

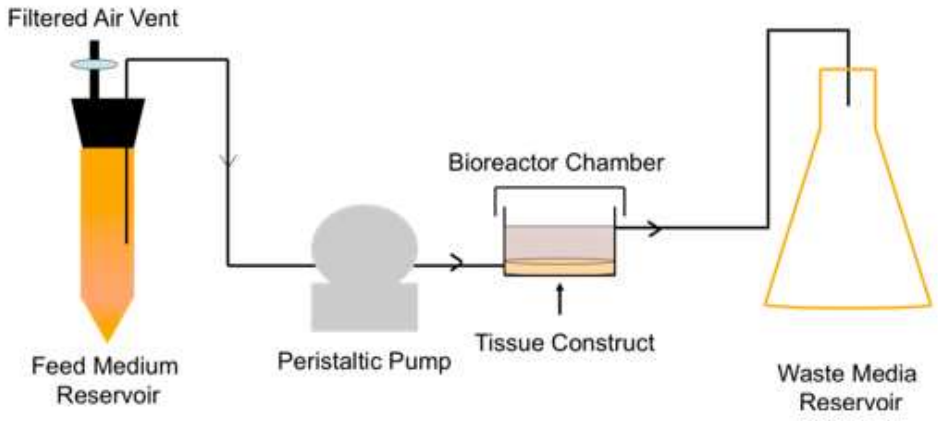


**Figure 3-1** The bioreactor system was composed of an 8-chamber polypropylene culture vessel with a vented lid to keep the chamber at atmospheric pressure (only one channel is shown for clarity) and a peristaltic pump to provide continuous media flow.

### 3.3.4 Effect of different seeding preparations.

To determine the most effective method to synthesize large cartilaginous constructs in reactor culture ($\geq 3$ cm$^2$) , three different preparations were investigated: (i) biopsy culture, (ii) monolayer culture, and (iii) cell pellet culture. Rabbit cartilage biopsies (3 mm diameter) were pretreated with 0.15% collagenase for 15 min to encourage cellular budding at the tissue edge[102]. Monolayer cultures involved seeding 20,000 isolated rabbit chondrocytes directly on the bottom surface of the reactor (~ 6500 cells/cm$^2$). Pellet cultures were formed by centrifuging 200,000 isolated cells for 10 min at 500 g[103]. After seeding, all preparations were maintained under no-flow conditions for 48 hours. Preparations were then cultured under a constant media flow rate of 10 μL/min for 5 weeks in Ham's F12 media (supplemented with 25 mM HEPES, 20% FBS, 15 mM

$NaHCO_3$, 100 μg/mL ascorbic acid and antibiotics). Media reservoirs were changed every 2-3 days and supplemented with fresh ascorbic acid and antibiotics. After 5 weeks, engineered constructs were harvested for visual, histological and immunohistochemical evaluation. Two separate trials of this study were conducted (minimum *n=2/group*).

### 3.3.5 Effect of bioreactor culture time.

To investigate the effect of culture time on construct development, additional cultures from the optimal preparation method determined in the previous study (monolayer culture) were established and cultivated for 2, 3 or 4 weeks to assess the effect of culture time on construct thickness, extracellular matrix (ECM) accumulation, histological/immunohistochemical evaluation, and mechanical properties. At each time point, harvested constructs were assessed for their thickness and mechanical properties. Constructs were then equilibrated in Ham's F12 media for one hour after mechanical testing and then cut in half. One half was used for biochemical analyses and the other half was used for histological and immunohistochemical evaluation. Two separate trials of this study were conducted for each time point (minimum *n=8/group*).

### 3.3.6 Thickness and mechanical properties of engineered constructs.

Cartilage construct thickness was determined using a needle probe method[104]. Harvested constructs were placed on a stainless steel stage coated in waterproof sand paper. A 25

ga. needle (Becton Dickinson, Franklin Lakes, NJ, USA) attached to a 1 kg load cell of a Mach-1 micromechanical tester (Biomomentum Inc., Laval, QC, Canada) was displaced into the tissue at a rate of 5 μm/s. Resistive compressive force and needle displacement were recorded at a frequency of 10 Hz. Abrupt changes in force were observed when the needle made contact with the tissue and then again when the needle made contact with the underlying support; and the difference was interpreted as the tissue thickness[104]. Construct thickness was measured twice at two random locations and averaged together. All measurements were conducted at 37°C with the constructs bathed in Ham's F12 media.

Construct mechanical properties (indentation modulus) were determined using a double indentation method[105,106]. This method uses the response from two separate indentations of different indenter sizes at the same site to determine the elastic modulus of the sample. Plane-ended indenters (2 mm and 6 mm diameter) attached to a 1 kg load cell of a Mach-1 micromechanical tester (Biomomentum Inc) were displaced into the tissue at a rate of 10% strain/s to a strain of 15%. The construct was allowed to equilibrate for 15 minutes between indentations. The instantaneous slope for both indentions was then used to calculate the instantaneous elastic modulus of the tissue according to the procedure outlined by Jin & Lewis[105].

### 3.3.7 Biochemical analyses of the accumulated ECM.

After mechanical property assessment, tissue constructs were weighed (wet weight) and cut in half. Tissue sections were weighed again (to determine the percentage mass of each section). The section used for biochemical analyses was processed as follows. Tissue samples were lyophilized overnight and then weighed (dry weight). Constructs were then digested by papain (80 μg/mL) and stored at -20°C until analysis. Aliquots of the digest were assayed separately for proteoglycan, collagen and DNA contents. The proteoglycan content was estimated by quantifying the amount of sulphated glycosaminoglycans using the dimethylmethylene blue dye binding assay[107,108]. Collagen content was estimated from the determination of the hydroxyproline content. Aliquots of the papain digest were hydrolyzed in 6 N HCl at 110ºC for 18 hours and the hydroxyproline content of the hydrolyzate was then determined using chloramine-T/Ehrlich's reagent assay[109]. Collagen content was estimated assuming hydroxyproline accounts for 10% of the total collagen mass in cartilage[110]. The DNA content was estimated using the Hoechst 33258 dye assay[101].

### 3.3.8 Histological and immunohistochemical evaluation.

The remaining half of the tissue constructs were further cut into two sections, with one half (1/4 of the total sample) for histological evaluation and the other (1/4 of the total sample) for immunohistochemical evaluation. For histological evaluation, the tissue sample was fixed in 4% paraformaldehyde (v/v) (Sigma-Aldrich) overnight at 4°C and

then stored in 70% ethanol (v/v) until further processing. Fixed samples were embedded in paraffin and thin sections (5 μM) were cut. Paraffin was removed by immersion in toluene, followed by immersion in a series of graded ethanol-water solutions to rehydrate the sections. Sections were stained with either Weigert's Iron hemotoxylin-eosin (H&E, a general connective tissue stain), toluidine blue (TB, to stain sulphated proteoglycans) and Masson's Trichrome (to stain collagen). After staining, sections were dehydrated by sequential immersion in alcohol, mounted with mounting medium, and examined by light microscopy.

The other 1/4 of the total sample was prepared for immunohistochemical evaluation. Samples were cryo-embedded in CryoMatrix™ (Thermo Scientific, Rockford, IL) and frozen solid in a methanol/dry ice bath. Cryo-sections 10 μm thick were cut on a cryostat at -25 °C and mounted on Superfrost Plus™ slides (Fisherbrand). Sections were enzymatically treated to facilitate antibody binding. The sections were first treated with 0.25 units/mL chondroitinase ABC (Sigma-Aldrich) in Tris-acetate buffer (40 mM Tris acetate with 1 mM EDTA), pH 8.5 for 1 hour at 37°C, and subsequently with 0.25 units/mL Keratanase (Sigma-Aldrich) Tris-acetate buffer (40 mM Tris acetate with 1 mM EDTA, pH 8.5) for 30 minutes at 37°C[111]. Sections were then immersed in 3% $H_2O_2$ (v/v) for 10 minutes to quench endogenous peroxidase activity[112]. To reduce non-specific protein binding, the sections were blocked with horse serum (Vector Laboratories Inc., Burlingame, CA, USA), in PBS (pH 7.4) for 30 minutes at room temperature. Type I

collagen sections were incubated with mouse monoclonal type I primary antibody (I-8H5: Daiichi Fine Chemicals Co Ltd, Japan) at 40 μg/mL in 10% serum (v/v) in PBS (pH 7.4) overnight at 4°C. Type II collagen sections were incubated with mouse monoclonal type II primary antibody (II-II6B3: Developmental Studies Hybridoma Bank, University of Iowa, IA, USA) at a 1:200 dilution in 10% horse serum (v/v) in PBS (pH 7.4) overnight at 4°C. Following primary antibody incubation, sections were rinsed in PBS (pH 7.4), and incubated with FITC secondary antibody (Vector Laboratories) with 10 % horse serum (v/v) in PBS with 0.1% Triton X-100 (v/v) for both type I and II collagen for 30 minutes at room temperature. Sections were counterstained and mounted with DAPI (Vector Laboratories) and examined by fluorescent microscopy. To assess non-specific staining, the primary antibody was omitted from each type of section.

### 3.3.9 Construct implantation study.

This study was performed with approval from the University Animal Care Committee (UACC) at Queen's University. New Zealand white rabbits (2 ± 0.3 kg) were anesthetized with medetomidine (0.2 mg/kg), butorphanol (1 mg/kg) and ketamine (10 mg/kg), administered intramuscularly. The surgeries were performed by Dr. Davide Bardana (Department of Surgery, Queen's University, Kingston, Canada). Rabbits were intubated and maintained on isoflurane (1.5-3%). The right hind leg of each rabbit was shaved and cleaned with a surgical scrub (2% choloxylenol antibacterial soap), alcohol and betadine. A 2 mg/kg dose of bupivicaine was infiltrated at the site of incision.

Throughout the surgical procedure, the animals were placed on a heating pad and vital signs were monitored, including heart rate and the saturation of peripheral oxygen ($S_PO_2$). The right knee was approached through a medial parapatellar incision and the patella was dislocated laterally to expose the tibiofemoral joint surface. A single 4 mm circular chondral-only critical-sized[25] defect was made using a biopsy punch (VWR International) in the trochlear groove, taking care not to penetrate the underlying subcondral bone. Allogenic engineered constructs were cut to size using a 4 mm biopsy punch and implanted in the defect site. Construct fixation was achieved by a combination of fibrin sealant (Tisseel, Baxter Corporation, Mississauga, ON) and three 8-0 prolene sutures (120 degrees apart: 2 anterior, 1 posterior) to ensure fixation to the subchondral bone and surrounding native tissue, respectively. Control defects were given fibrin sealant and then left untreated. The patella was repositioned and the joint was articulated several times. The joint capsule was closed with monocryl 4-0 interrupted suture pattern, and the skin was closed with 4-0 Nylon using a simple interrupted pattern. After surgery, analgesics were administered sub-cutaneously: meloxicam (0.3 mg/kg) for 5 days and buprenorphine (0.05 mg/kg) for 3 days. Animal care and handling was performed by Debbie Harrington (Queen's veterinary services). Post-surgery the animals were scored daily for pain and behaviour over seven days. The animals were euthanized after one month for evaluation.

After euthanization, the joint was opened and the repair site scored using the ICRS Macroscopic Scoring system (Appendix B, Figure B1)[113]. Macroscopic scoring was

performed unblinded by myself and Dr. Yat Tse (Department of Biomedical and Molecular Science, Queen's University, Kingston, Canada). The repair site was cut in half, one half for biochemical evaluation and the other half for histological/immunohistochemical evaluation. For biochemical analyses, half of the implanted construct was carefully removed along with a separate section of surrounding native cartilage using a No.11 scalpel. The samples were analyzed for DNA, proteoglycan and collagen contents, as described previously. Similarly, the remaining portion of the construct used for each implant was saved after surgery (stored at -20C) and analyzed to assess biochemical remodeling during implantation, as described previously. For histological/immunohistochemical evaluation, the remaining half of the defect site (implant and surrounding native tissue) and underlying bone was removed. The sample was fixed with 4% paraformaldehyde (w/v) over 72 hours and decalcified in 10% EDTA (w/v) (pH 6.5, Sigma-Aldrich) over a 5 week period at room temperature on an orbital shaker with solution changed twice per week. The decalcified tissue samples were embedded in paraffin and thin sections (5 μm) were cut. Paraffin was removed by immersion in toluene, followed by immersion in a series of graded ethanol-water solutions to rehydrate the sections. The sections were then assessed histologically (as described previously) or immunohistochemically, using the same procedure described previously but using a different detection system for paraffin embedded sections. Following primary antibody incubation, sections were rinsed in PBS (pH 7.4), and incubated with biotinylated secondary antibodies using the Vectastain® Elite ABC kit

(Vector Laboratories) with 10% horse serum (v/v) in PBS. Immunodetection was performed using 3, 3'-diaminobenzidine tablets (Sigma-Aldrich) for colour development according to the ABC kit instructions. Sections were counterstained with nuclear fast red stain for 10 seconds. Sections were then cleared and dehydrated by immersion in water and a series of graded alcohol, mounted with mounting medium and examined by light microscopy. To assess non-specific staining, the primary antibody was omitted from each type of section.

### 3.3.10 Mold formation and creation of patient-specific constructs.

Patient-specific chondral constructs were generated in the shape and curvature of an existing cartilage defect using rapid-prototyped molds of imaged joint surfaces conducted by Dr. Manuela Kunz (Human Mobility Research Centre, Queen's University and Kingston General Hospital). In a previous study, blunt-force trauma defects were produced in the medial femoral condyle of skeletally mature Suffolk-Dorset sheep which were then allow to degenerate into irregularly shaped defects over a period of three months[114]. A 3D computer model of the stifle joint containing the cartilage defect was then generated from computed tomography (CT) arthrogram imaging (GE Healthcare LightSpeed Plus) followed by segmentation of the cartilage and bone surfaces. The surface geometry of the cartilage defect (shape and curvature) was then extracted from the 3D model and incorporated into a cylindrical mold (19 mm OD to fit within the reactor), which was then fabricated by rapid prototyping out of non-cytotoxic,

acrylonitrile butadiene styrene (ABS) thermoplastic (Stratasys Dimension SST 1200 es). Mold surfaces were first coated with 100μL of 0.5 mg/mL type II collagen (Sigma-Aldrich) and then seeded at a density of 6,700 cells/cm$^2$ (2,500 cells per mold). After seeding, cell-seeded molds were maintained under no-flow conditions for 48 hours. Mold cultures were then cultured under a constant media flow rate of 10 μL/min for 3 weeks in Ham's F12 media (supplemented with 25 mM HEPES, 20% FBS, 15 mM $NaHCO_3$, 100 μg/mL ascorbic acid and antibiotics). Media reservoirs were changed every 2-3 days and supplemented with fresh ascorbic acid and antibiotics. After 3 weeks, engineered patient-specific constructs were harvested to assess shape fidelity ($n$=4) and histological/immunohistochemical evaluation ($n$=1).

After harvest, the surface morphology of both the construct and mold were measured using a 3D laser scanning system (ShapeGrabber SG2 Series), conducted by Dr. Manuela Kunz (Human Mobility Research Centre, Queen's University and Kingston General Hospital). As the construct was slightly transparent, a thin layer of white aerosol deodorant was sprayed on the surface of the construct prior to scanning. Shape fidelity of the engineered patient-specific construct was evaluated by determining the root mean square (RMS) error between the mold and construct surfaces using an iterative closest point (ICP) matching algorithm[115]. Constructs were also harvested for histological/immunohistochemical evaluation as described previously.

### 3.3.11 Statistical analyses.

Each experimental group had a sample size of at least 4 and typically ranged from 6-8. *In vitro* experiments were repeated at least twice using chondrocytes from different rabbits and the combined data were analyzed. All results were expressed as the normalized mean ± standard error of the mean (SEM). Collected data were analyzed statistically using a one-way analysis of variance (ANOVA) and the Fisher's least significant difference (LSD) post-hoc test (SPSS version 16, SPSS Inc., Chicago, IL, USA) to determine the effect of $NaHCO_3$ concentration and culture time. The data were checked prior to performing statistical tests for both normality and equal-variance. Significance was associated with $p$-values less than 0.05 and trends were noted with $p$-values between 0.05 and 0.1.

## 3.4 Results and Discussion

### 3.4.1 Determination of optimal sodium bicarbonate concentration.

Isolated rabbit chondrocytes seeded in 3D agarose cultures were established to determine the optimal concentration of sodium bicarbonate for subsequent bioreactor culture. The cell seeded agarose cultures were maintained in media containing varying concentrations of sodium bicarbonate ($NaHCO_3$; 0, 15, 20, 25 or, 30mM) for two weeks. The supplementation of media with $NaHCO_3$ elicited significant effects in terms of extracellular matrix synthesis and DNA content ($p<0.05$) (Figure 3-2). Collagen synthesis was increasingly up-regulated under increasing $NaHCO_3$ concentration (by 41 – 67%). The effect on proteoglycan synthesis followed a similar trend with increasing $NaHCO_3$ concentration (by 45 – 50%). $NaHCO_3$ supplementation also resulted in significant increases in DNA content (by 84 – 122%). As $NaHCO_3$ supplementation had the greatest effect between the concentrations of 0 and 15 mM, a 15mM concentration $NaHCO_3$ was used for bioreactor culture.

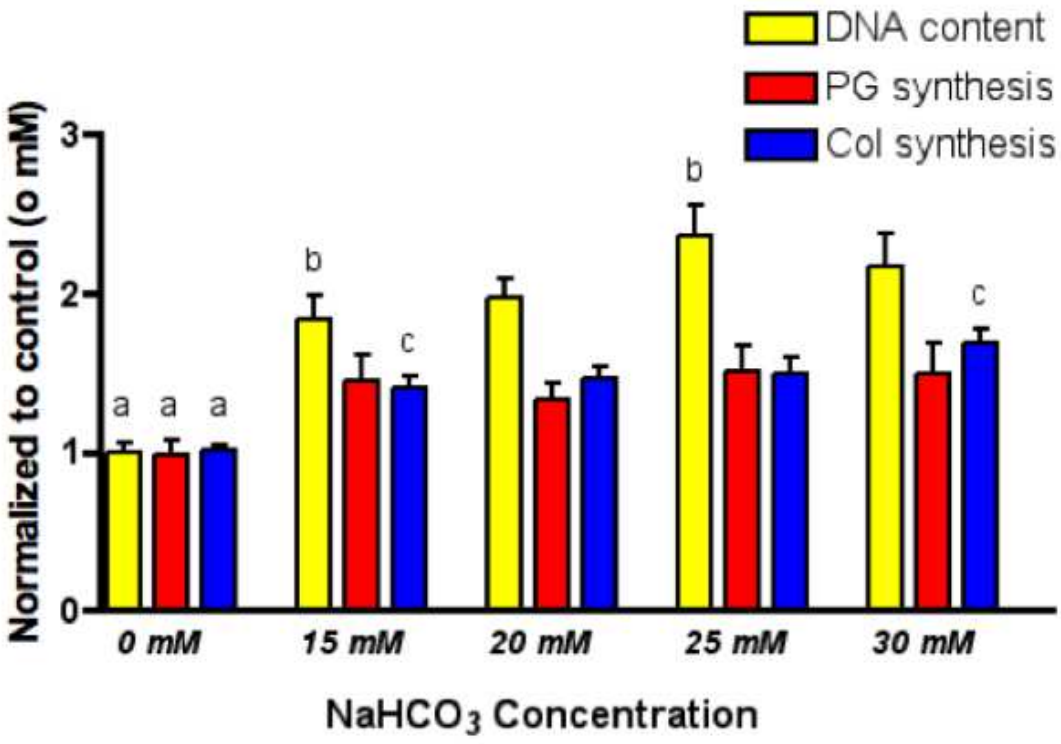


**Figure 3-1 Effect of $NaHCO_3$ concentration on ECM synthesis and DNA content**. Data from several experiments are pooled together and presented as mean ± SEM normalized to the control (0 mM). Proteoglycan and collagen synthesis were normalized to DNA content ($n$=10-12 samples/group). [a] significantly different from all other groups ($p<0.05$), [b,c] significantly different from one another ($p<0.01$).

### 3.4.2 Development of cartilaginous tissue constructs.

Large-sized engineered cartilage constructs (≥ 3 $cm^2$) were developed in the bioreactor for a period of 5 weeks under a constant flow of fresh culture media. To demonstrate the versatility of this approach, engineered tissue constructs were produced from three different preparations of extracted tissue or cells using the minimal bicarbonate concentration to stimulate tissue growth: (i) cartilage biopsies (3 mm in diameter)

pretreated with collagenase to encourage cellular budding at the tissue edge[102], (ii) an equivalent number of isolated chondrocytes (~ 20,000 cells) seeded in monolayer, and (iii) isolated chondrocyte pellets (~ 200,000 cells). All tissue and cell preparations were harvested from the femoral condyles of New Zealand White rabbits (2 ± 0.5 kg). Each of the three methods resulted in the formation of large-sized tissue constructs (≥ 3 $cm^2$) with a hyaline-like appearance. While the tissue generated from the monolayer and pellet preparations covered the entire bottom of the reactor well, inconsistent tissue growth was observed with biopsy preparations (Figure 3-3 a). Histological and immunohistochemical staining of the generated tissues confirmed the formation of cartilaginous ECM noted by the presence of sulphated proteoglycans (Figure 3-3 b) and type II collagen (Figure 3-3 c). While all of the generated tissues exhibited regional staining for type I collagen (Figure 3-3 d), type I collagen appeared to be primarily concentrated at the bottom surface of the construct. This effect was more pronounced in the tissues generated from a cartilage biopsy as opposed to those generated from isolated cells (monolayer or pellet preparations). While type I collagen is minimally expressed in the deep zone of native cartilage[24], the presence of type I collagen in the generated tissues was most likely due to local dedifferentiation of the cells that were intimately in contact with the reactor well surface[24]. As the monolayer constructs required the least number cells and was able to produce tissue constructs of uniform thickness and shape, this method was employed for all subsequent studies.

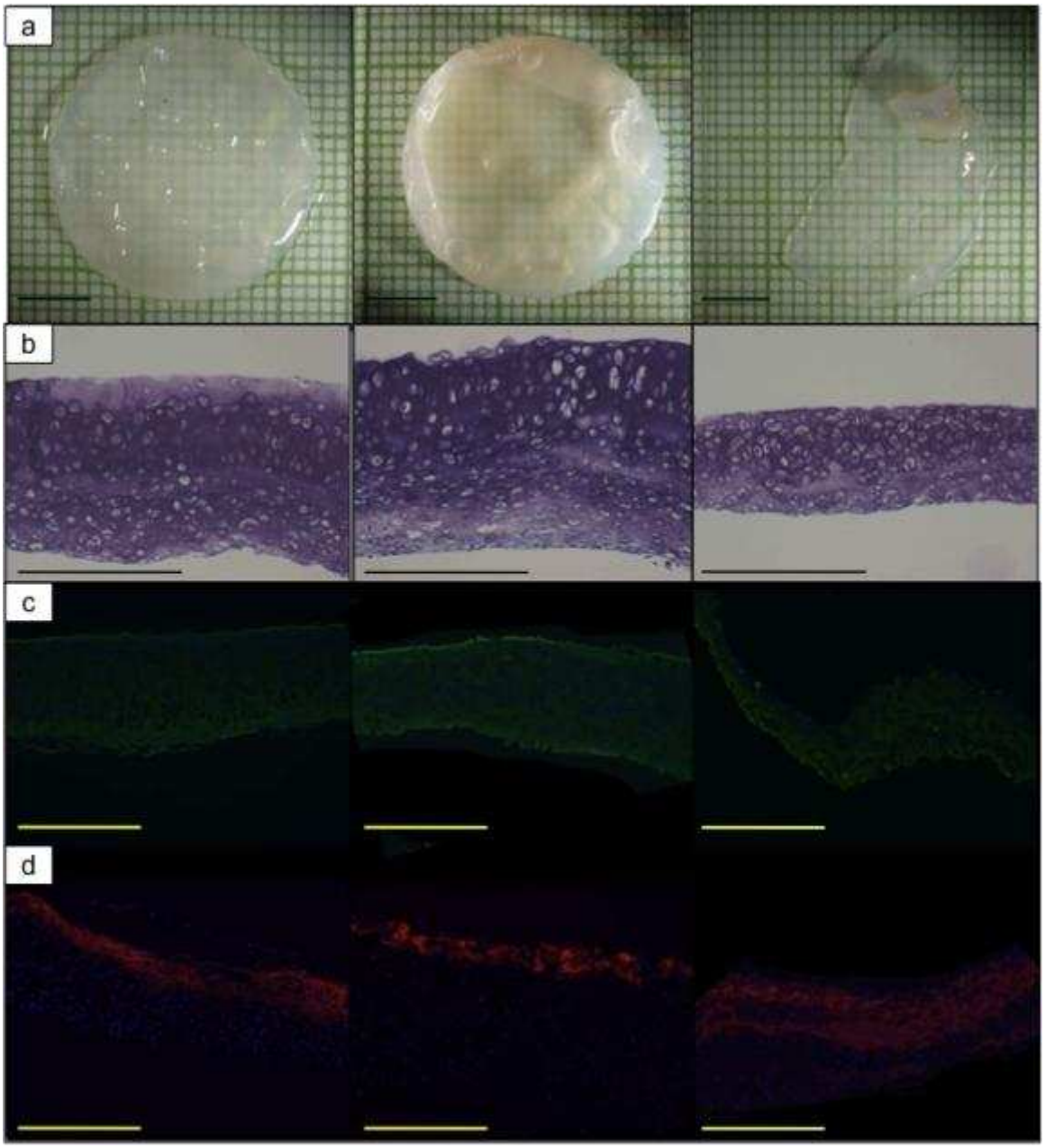


**Figure 3-3 Effect of seeding method on the generation of large-sized cartilaginous tissues.** A) Macroscopic appearance of the tissue generated from the monolayer, pellet and biopsy preparations after 5 weeks of bioreactor culture. B) Toluidine blue staining (sulphated proteoglycans) of the tissues generated from each preparation. C) Immunohistochemical staining of the tissues generated from each preparation for type II collagen. D) Immunohistochemical staining of the tissues generated from each preparation for type I collagen. Scale bar represents 0.5 mm for (panel A) and 300 μm for (panels B-D).

### 3.4.3 Effect of culture time.

A study was conducted to determine the optimal culture length in order to generate large-sized cartilaginous tissues ($\geq 3$ cm$^2$) closely matched to the thickness and properties of native cartilage. Increasing culture time had a positive effect on tissue thickness and was greatest between weeks 2 and 3 of culture (Table 3-1). The obtained tissue thickness of the engineered constructs fell within the range of rabbit knee articular cartilage (0.2 - 0.4 mm)[38,116]. Biochemical analysis of the synthesized ECM and DNA content exhibited a similar pattern, indicating significant ECM accumulation and cellular proliferation between weeks 2 and 3 of culture (Table 3-1). As the changes in tissue proteoglycan content with culture time were not as pronounced as the increases in collagen content, significant increases in the collagen:proteoglycan ratio were observed with increasing culture time (68% increase between weeks 2 and 4; Table 3-1). Although increasing maturation of the engineered tissues were observed with longer culture times, these values were still below those typically reported for native articular cartilage (2:1 to 3:1 collagen:proteoglycans)[117,118]. The observed changes in tissue biomechanical properties (indentation modulus) mirrored the changes in ECM deposition with increasing properties observed up to week 3 and remained constant with longer culture times (Table 3-1). Similarly, although culture time had a positive effect on tissue biomechanical properties, measured moduli were lower compared to native articular cartilage (aggregate modulus for rabbit patellar groove ~0.516 MPa)[75,77]. Histological and immunohistochemical assessment of the generated cartilaginous tissues also revealed increasing ECM deposition with increasing culture time (Figure 3-4).

**Table 3-1 Physical, biochemical and biomechanical properties of engineered large-sized cartilaginous tissues**. Two separate experiments were performed, results pooled, and data presented as mean ± SEM (*n* = 6-8 samples/group).

| | Week 2 | Week 3 | Week 4 |
|---|---|---|---|
| **Water Content (%)** | 90.2 ± 0.5 | 91.1 ± 0.3 | 91.1 ± 0.2 |
| **DNA(μg)** | 14 ± 1[a] | 30 ± 2 | 35 ± 3 |
| **GAG(μg)** | 1868 ± 155[c] | 2854 ± 215 | 3367 ± 447 |
| **Collagen(μg)** | 536 ± 68[a] | 1122 ± 128[a] | 1496 ± 104[a] |
| **Collagen/GAG** | 0.30 ± 0.05 | 0.40 ± 0.05[b] | 0.51 ± 0.08[c] |
| **Thickness (mm)** | 0.26 ± 0.02[a] | 0.42 ± 0.04 | 0.44 ± 0.03 |
| **Indentation Modulus (KPa)** | 5 ± 1[d] | 13 ± 2[d] | 12 ± 2[b] |

[a] significantly different from all other groups ($p<0.01$)
[b] trend ($0.1>p>0.05$) from week 2
[c] significantly different from all other groups ($p<0.05$)
[d] significantly different from one another ($p<0.01$)

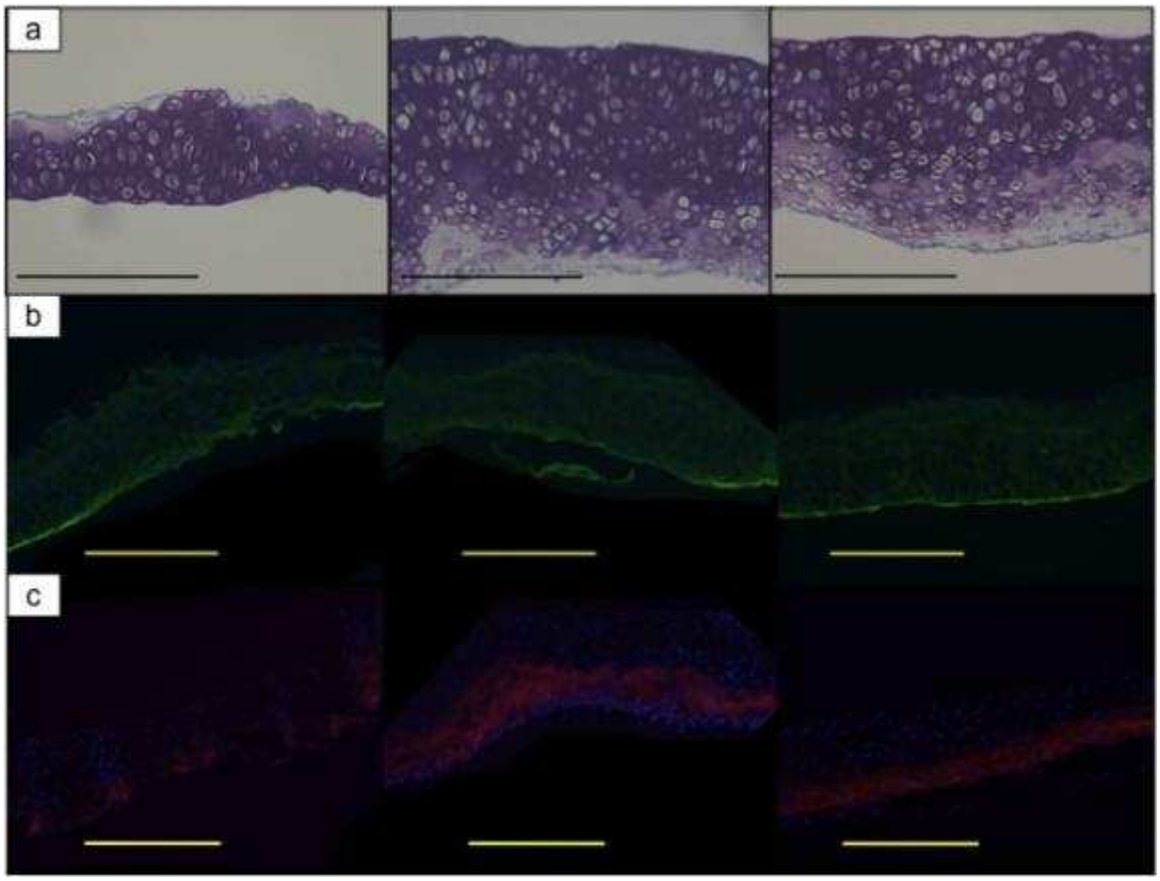


**Figure 3-4 Effect of culture time on the generation of large-sized cartilaginous tissues**. A) Toluidine blue staining (sulphated proteoglycans) of the tissues generated after 2 (left), 3 (middle) and 4 (right) weeks of bioreactor culture. B) Immunohistochemical staining of the tissues generated from each time point for type II collagen. C) Immunohistochemical staining of the tissues generated from each time point for type I collagen. Scale bar represents 300 μm for all panels.

### 3.4.4 Ability of the engineered tissue constructs to survive implantation.

To determine whether the generated large-sized tissue constructs ($\geq 3$ $cm^2$) were able to survive *in vivo*, a small allogenic implantation study was conducted in rabbits for a period of 4 weeks. A 4 mm critical-sized full thickness chondral (cartilage only) defect was established in the trochlear groove of the knee in New Zealand White rabbits ($2 \pm 0.5$ kg)

which was larger than that reported for spontaneous tissue repair (< 3 mm)[25]. Care was taken not to penetrate the underlying subchondral bone, thereby eliminating the presence of exogenous repair factors. Allogenic tissue constructs were secured in place with fibrin glue and three sutures placed around the periphery of the graft. A sham knee was also created using the addition of fibrin glue alone. After implantation there was no sign of chronic inflammation in the treated knees over the 4 week post-operative period. Macroscopic evaluation of the treated defects revealed complete defect filling with tissue that was similar in colour and texture to the surrounding native cartilage in 3 of the 4 defects (Figure 3-5 a). These three grafts were smooth and level with the surrounding native cartilage and received near perfect scoring (mean ICRS score: 11.7 out of 12). The surface of the fourth defect was irregular and filling was inconsistent, suggesting that the implant was lost (ICRS score 3 out of 12). For the sham knee, there was the presence of tissue within the defect, which was irregular and covered only about 50% of the defect surface area (ICRS score: 4). Macroscopically, the defect boundaries for the implant knees could barely be distinguished from the native cartilage, suggesting good integration between the engineered graft and the surrounding cartilage. Histological evaluation of the three implanted constructs confirmed excellent integration of the implant with surrounding native cartilage and good fixation to the underlying subchondral bone (Figure 3-5 b). In addition, the implanted tissues appeared to structurally remodel towards that of native cartilage by displaying the characteristic cellular architecture of columnar cells in the deeper zones accompanied with flattened cells at the implant surface (Figure

3-5 b). Evaluation of the sham operated knee indicated minimal filling of repair tissue with no apparent cellular organization (Figure 3-5 b). The implanted tissue grafts also appeared to retain their phenotype by exhibiting type II collagen expression throughout the tissue with minimal expression of type I collagen (Figures 3-5 c-d). Biochemical evaluation of retrieved grafts supported the observation of construct remodeling post-implantation with the graft tissues adopted accumulation of ECM similar to that of the surrounding native cartilage (Table 3-2).

**Table 3-2** Implantation on large-sized engineered constructs 4 weeks post-implantation. Data presented as mean ± SEM ($n$ = 4).

| | **Native** | **Implant** |
|---|---|---|
| **DNA(μg)/ Dry weight (mg)** | 4.1 ± 0.1[a] | 6.4 ± 0.8[a] |
| **GAG(μg)/ Dry weight (mg)** | 145 ± 8 | 111 ± 22 |
| **Collagen(μg)/ Dry weight (mg)** | 320 ± 84 | 326 ± 99 |
| **Collagen/GAG** | 3.1 ± 0.1 | 4.0 ± 0.4 |

[a]significantly different from one another ($p<0.05$)

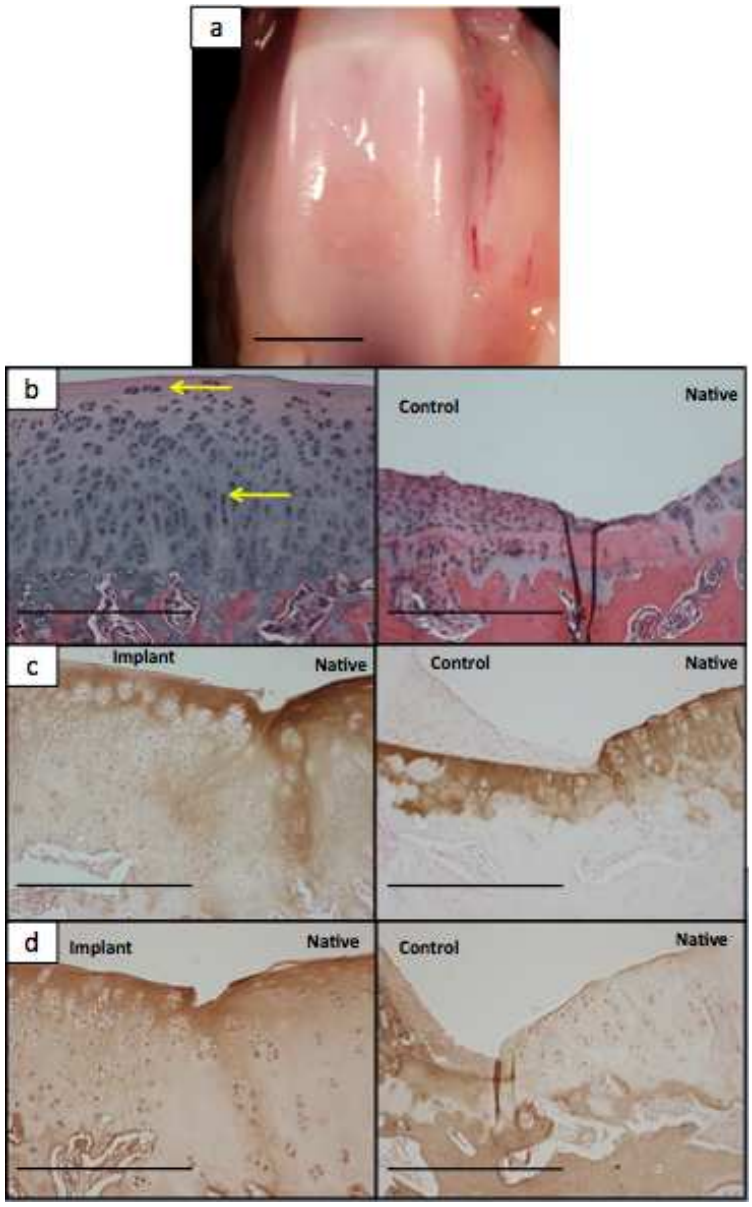


**Figure 3-2 Implantation on large-sized engineered constructs 4 weeks post-implantation**. A) Macroscopic appearance of the repaired defect site in the rabbit trochlear groove 4 weeks post-operative. B) Hematoxylin and eosin (H&E) staining of the implanted tissue (10X) (left) and sham (unoperated) defect (10X) (right). Yellow arrows indicate flattening of the surface cells and columnar formation of the deeper zone chondrocytes. C) Immunohistochemical staining of the implanted tissue (10X) (left) and sham (unoperated) defect (10X) (right) for type II collagen. D) Immunohistochemical staining of the implanted tissue (10X) (left) and sham (unoperated) defect (10X) (right) for type I collagen. Scale bar represents 0.4 mm for (panel A) and 300 μm for (panels B-D).

### 3.4.5 Development of patient-specific constructs.

As the synthesized tissue appeared to adopt the shape of the reactor vessel, rapid-prototyped defect molds were used to explore the possibility of generating constructs matched to the shape and surface geometry of the patient's anatomy. After three weeks in culture, isolated chondrocytes seeded into the fabricated defect molds (6,700 cells/cm$^2$ or ~2,500 cells per mold) were able to synthesize cartilaginous tissue constructs that conformed to the size, shape and curvature of the mold (Figure 3-6 a). Shape fidelity of the constructs was preserved as there was good agreement between the construct and mold surfaces with an average error (root mean square) of 114 ± 2 μm ($n$ = 4, Appendix C, Figure C1). The majority of the patient-specific construct surface was within 50 μm of the mold with regions of higher deviation noted primarily at the edges of the construct (Figure 3-6 b). Histological and immunohistochemical assessment of the generated patient-specific tissue constructs also revealed no apparent influence of the mold materials on tissue structure or phenotype (Figures 3-6 c-d). These results demonstrate that scaffold-free engineered constructs can be tailored to match the geometry of an existing defect which is a significant advantage over the current methodology that uses generically shaped scaffolds to incorporate anatomical features in the generated engineered grafts[119,120].

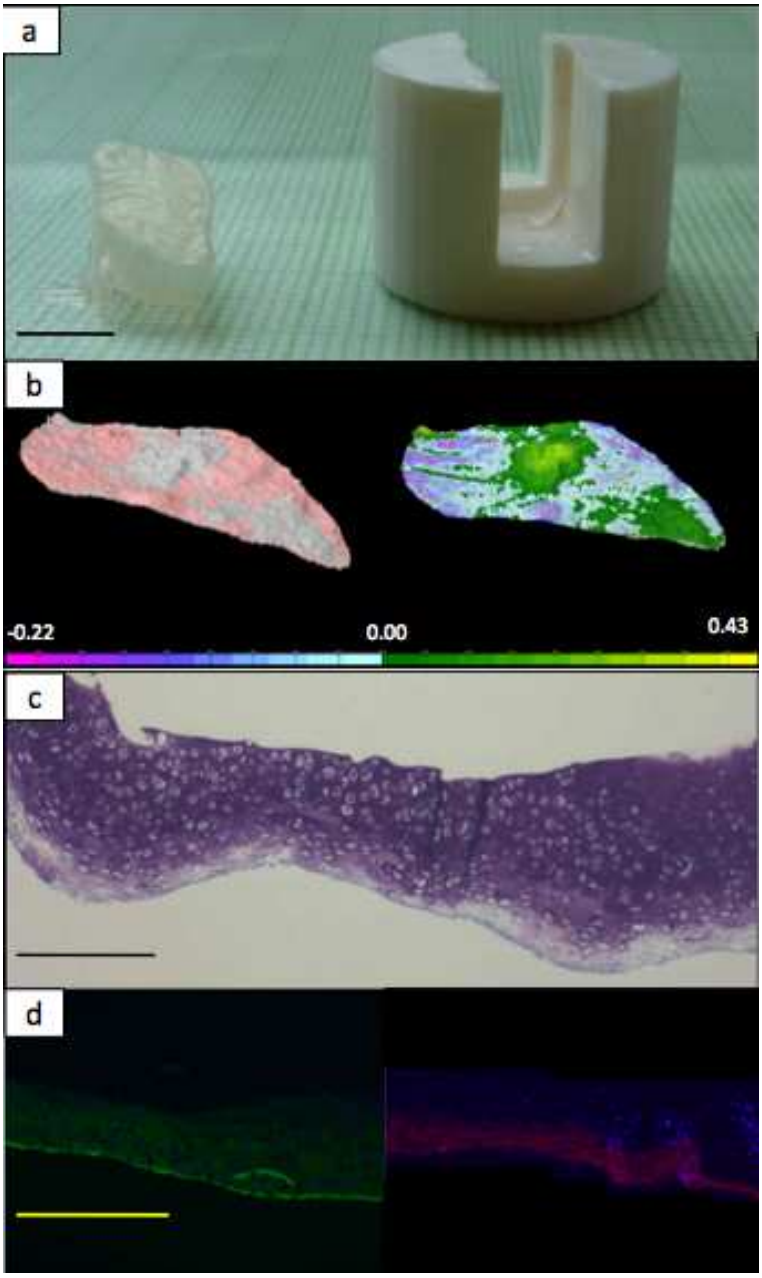


**Figure 3-3** Development of patient-specific cartilaginous tissue constructs. A) Macroscopic appearance of the defect mold (right) alongside the resulting cartilaginous construct (left) after 3 weeks of bioreactor culture. B) Distance map between the surface of the mold (left) and the patient-specific construct (right). C) Toluidine blue staining (sulphated proteoglycans) of the patient-specific constructs. D) Immunohistochemical staining of the patient-specific constructs for type II collagen (left) and type I collagen (right). Scale bar represents 0.5mm for panel (A), -0.22 mm to 0.43 mm for panel (B) and 300 μm for panels (C-D). Distance map units are in mm.

## 3.5 Conclusions

With an ever-increasing aging population, the demand for regenerative strategies will continue to increase. In terms of cartilage, tissue damage as a result of trauma or osteoarthritis is a substantial healthcare burden which affects 1 in 10 individuals[121]. Current treatment algorithms are limited by either an inferior quality of generated repair tissue (e.g. microfracture) or the amount of available donor tissue (e.g. mosaic arthroplasty and ACI)[9]. These indicate a need for improved strategies for cartilage repair and reconstruction. An approach to generate phenotypically-stable, large-sized tissue engineered cartilage constructs ($\geq 3$ cm$^2$) without the use of a cell expansion phase or a scaffold was described in this study. The approach uses a very small population of isolated cells to stimulate the extensive growth of new cartilaginous tissue. This represents a significant clinical advantage as only a small amount of donor tissue is required, which is approximately 20 times less than what is typically required for ACI[13]. This approach represents a significant shift from the current cartilage tissue engineering paradigm, as it has been shown that cartilaginous tissue constructs can essentially be generated from over-confluent monolayers which are generally believed to elicit cellular dedifferentiation and the production of poor quality, non-hyaline-like tissue.

In addition to the ability to produce large-size engineered cartilage constructs ($\geq 3$ cm$^2$) from a limited supply of donor cells, the generated tissue constructs were able to adopt both the structure and biochemical composition of native cartilage constructs after

implantation; thereby indicating that long-term viability and function are within reach. This result is a significant improvement for traditional cartilage tissue engineering approaches which have proven difficult to recapitulate the structure and cellular architecture of native articular cartilage. The versatility of the approach is further highlighted by the ability to synthesize tissue grafts matched to the anatomy of the patient. Through the use of non-invasive imaging, defect molds can be created to guide tissue formation to create tailored patient-specific constructs leading to improved restoration of the joint surface.

The bioreactor cultivated cartilaginous tissue constructs were similar in terms of thickness, proteoglycan content and DNA content to that of native articular cartilage. However, the accumulation of collagen and resultant mechanical properties were not at the level of native cartilage. Future studies will investigate methods to further mature the tissue constructs during development which may be necessary for successful implantation in more mechanically demanding environments, such high weight-bearing regions of the femoral condyles. Also, as only chondral (cartilage only) constructs have been developed so far, cartilage defects that have bony involvement would not be candidates for repair thereby limiting the clinical utility of this approach. However, this treatment could be expanded to develop large-sized, engineered osteochondral grafts with the use of bioreactor cultivated tissue incorporated on the surface of bone-substitute materials.

This study has outlined an approach to generate large-size cartilaginous tissue grafts from a limited supply of donor cells that also can survive full weight bearing in the repair critical-sized cartilage defects. The implanted tissues were observed to remodel, both structurally and biochemically, towards that of native cartilage after a relative short period *in vivo*. It has also demonstrated the potential of growing tissue constructs matched to the anatomy at the defect site leading to more accurate reconstruction of the articular surface. To ensure clinical success of this new approach, future studies need to be conducted in a larger animal model with pre-existing defects to evaluate long-term effectiveness in cartilage repair.

# Chapter 4

# Repair of Chondral Defects with Scaffold-free Engineered Cartilage Constructs in a Rabbit Model

## 4.1 Abstract

The absence of spontaneous healing in purely chondral defects is compounded by articular cartilage's limited ability for self-repair. The objective of this study was to generate in *vitro* scaffold-free cartilage constructs to facilitate *in vivo* repair of chondral defects. Isolated rabbit chondrocytes were cultured in low density monolayers in a continuous-flow bioreactor to generate tissue constructs, which were then implanted into the patellar groove of immature New Zealand white rabbits. Fibrin glue and sutures were employed to ensure implant fixation, with control defects receiving fibrin glue alone. At 1, 3 and 6 months post-implantation, explanted knees were assessed macroscopically, histogically and biochemically to evaluate the extent of repair and integration. The majority of the defects received macroscopic scores (ICRS) that correspond to nearly normal repair (>8). Histological analyses of implanted engineered constructs revealed hyaline-like repair tissue, as well as good integration to the adjacent cartilage. Immunohistochemical analyses showed homogeneous distribution of collagen type II with minimal presence of collagen type I. Biochemical evaluation of the repair tissue revealed extensive *in vivo* remodeling and was superior to control repair tissue at every

time point. In addition, after 3 months post-operatively, DNA content and the collagen to proteoglycan ratio of the repair tissue were similar to that of the surrounding native cartilage. Repair of the chondral defects with the large-sized engineered constructs ($\geq 3$ $cm^2$) yielded consistent repair tissue up to 6 months post-implantation. With implantion, the constructs were predominantly composed of type II collagen and remodeled structurally and biochemically towards native articular cartilage. This repair strategy employs a unique culture method and shows promising results for future cartilage repair.

## 4.2 Introduction

The resilience of articular cartilage is compromised in two main ways- injury or disease. Damaged cartilage has a limited capacity for self-repair and this response will be influenced by the type of cartilage defect: chondral or osteochondral. While osteochondral defects can result in spontaneous repair, several studies have demonstrated that purely chondral defects do not necessarily heal on their own[1,82,122]. Damage to the articular cartilage surface is a common occurrence among professional and recreational athletes. These injuries result in altered joint function and discomfort, predisposing the individual to further cartilage degeneration and loss of joint function[31,71].

To circumvent articular cartilage's poor intrinsic repair capacity, several cartilage resurfacing strategies have been explored, such as filling the defect site with cells (autologous chondrocyte implantation) or with autologous grafts (mosaic arthroplasty) [83,69,9,39,38]. While good short-term results have been achieved, these repair strategies are characterized with inconsistent findings over the long-term[9,16]. As such these current techniques are thought as more palliative treatments, allowing for ease of pain rather than complete joint function restoration. In severe cases of cartilage degeneration, patients may require total joint replacement[5,48,82]. However, the long-term application of prosthetic joints is jeopardized by frequent failure rates[123]. With an ever-increasing aging population and substantial economic requirements for current short-term repair strategies, recent focus has turned towards regenerative techniques. Tissue engineering offers the

promise of a long-term, viable tissue replacement that is hyaline-like in appearance and can restore normal tissue function. Current tissue engineering techniques often employ three dimensional scaffolds to maintain chondrocytic phenotype[9]. Alternatively, recent observations have established that chondrocytes cultured in high-density can form their own matrix while retaining chondrogenic phenotype[61,124,125], thereby eliminating the need for a scaffold and avoiding scaffold-related issues (biocompatibility, toxicity, etc) [61].

Initial attempts to engineer articular cartilage have resulted in the generation of homogeneous tissue constructs for cartilage repair[23]. Given the unique structural organization of articular cartilage into distinct zones, it is unclear whether a homogeneous construct could adequately serve to replace, or repair, native cartilage. In a previous study, large-sized engineered constructs (>3cm$^2$) were synthesized from a relatively small amount of cells (20,000 per construct) without the use of a scaffold. Modifying culture time in this system has resulted in varying stages of architectural remodeling of the generated tissue constructs. As early as three weeks, zonal organization within the engineered construct was apparent and tissue thickness mirrored that of native cartilage. Thus, the purpose of the present study is to examine the *in vivo* performance of these engineered constructs implanted in a critical-sized chondral defect (> 3 mm[126,127]) and to investigate their reparative capacity over a period of six months post-operatively.

## 4.3 Materials and Methods

### 4.3.1 Rabbit chondrocyte harvest and isolation.

Full thickness articular cartilage was harvested from the femoral condyles of young female New Zealand white rabbits (2 ± 0.5 kg) (Charles River, Wilmington, MA). Chondrocytes were isolated from the extracted tissue by digestion with 0.5% protease (w/v) (Sigma-Aldrich, Oakville, ON) followed by 0.15% collagenase A (w/v) (Roche Diagnostics Canada, Laval, QC) in Ham's F12 media (Hyclone, Logan, UT, USA) supplemented with 25 mM HEPES (4-2(2-hydroxyethyl)piperazine-1-ethanesulfonic acid) (Sigma-Aldrich) and an antibiotic solution containing: 100 U/mL penicillin, 100 μg/mL streptomycin and 0.25 μg/mL amphotericin B (Sigma-Aldrich)[97] overnight at 37°C with 95% relative humidity and 5% $CO_2$. Cell viability was then determined by Trypan Blue dye (Sigma-Aldrich) exclusion[98].

### 4.3.2 Cartilaginous construct preparation.

The isolated chondrocytes were seeded into the wells of a continuous flow bioreactor[90,91] at a density of 20,000/well (~ 6500 cells/$cm^2$) in 1 mL of Ham's F12 media (supplemented with 25 mM HEPES, 20% FBS, 15 mM $NaHCO_3$, 100 μg/mL ascorbic acid and antibiotics). Cells were then cultured under a constant media flow rate of 10 μL/min for a period of 3 weeks to generate a continuous layer of cartilaginous tissue. Media reservoirs were changed every 2-3 days and supplemented with fresh ascorbic acid

and antibiotics. The bioreactor was housed in an incubator maintained at 37°C with 95% relative humidity and 5% $CO_2$ (Appendix A, Figure A 1). Tissue constructs were generated from different batches of isolated cells, which were used in the *in vivo* implantation study (six batches in total).

### 4.3.3 Construct implantation study.

This study was performed with approval from the University Animal Care Committee (UACC) at Queen's University. Twenty-three New Zealand white rabbits (2 ± 0.3 kg) were assigned randomly to three treatment groups: 1 month, 3 month, 6 month and control. The surgeries for this study were performed by Dr. Stephen Pang (Department of Biomedical and Molecular Science, Queen's University, Kingston, Canada). Rabbits were anesthetized with medetomidine (0.2 mg/kg), butorphanol (1 mg/kg) and ketamine 10 mg/kg), administered intramuscularly. Rabbits were then intubated and maintained on isoflurane (1.5-3 %). The right hind leg of each rabbit was shaved and cleaned with a surgical scrub (2% choloxylenol antibacterial soap), alcohol and betadine. A 2 mg/kg dose of bupivicaine was infiltrated at the site of incision. Throughout the surgical procedure, the animals were placed on a heating pad and vital signs were monitored, including heart rate and the saturation of peripheral oxygen ($SpO_2$). The right knee was approached through a medial parapatellar incision and the patella was dislocated laterally to expose the tibiofemoral joint surface. A single, 4 mm circular chondral-only critical-sized[25] defect was made using a biopsy punch (VWR International) in the trochlear

groove, taking care not to penetrate the underlying subcondral bone. Allogenic engineered constructs were cut to size using a 4 mm biopsy punch and implanted in the defect site. Construct fixation was achieved by a combination of fibrin sealant (Tisseel, Baxter Corporation, Mississauga, ON) and three 10-0 prolene sutures (120 degrees apart: 2 anterior, 1 posterior) to ensure fixation to the subchondral bone and surrounding native tissue, respectively. Control defects were given fibrin sealant and left untreated. The patella was repositioned and the joint was articulated several times. The joint capsule was closed with monocryl 4-0 interrupted suture pattern, and the skin was closed with 4-0 Nylon using a simple interrupted pattern. After surgery, analgesics were administered subcutaneously: meloxicam (0.3 mg/kg) for 5 days and buprenorphine (0.05 mg/kg) for 3 days. A functional evaluation of each animal post-implantation was performed daily, for up to seven days. Seven parameters including standing, gait, pain, swelling, incision appearance, body temperature and behavior, were scored between 0 (full recovery) and 3 (limited recovery)[128]. Additionally, blood was sampled from each rabbit to assess white blood cell counts. Seven to eight animals per observation time point were used: defects repaired with cartilaginous tissue constructs ($n$=6 per time point) or control with fibrin glue alone ($n$=2 for 1 and 3 month, $n$=1 for 6 month). After the repair period, animals were euthanized by a lethal overdose of sodium pentobarbital (100 mg/kg), the joint capsule opened, and the repair site scored using the ICRS Macroscopic Scoring system (unblinded by myself and Dr. Yat Tse)[129]. The repair site was then cut in half; one half

for biochemical evaluation and the other half for histological/immunohistochemical evaluation.

### 4.3.4 Biochemical analyses of the native and implant tissue.

For biochemical analyses, half of the implanted construct was carefully removed along with a separate section of surrounding native cartilage using a No.11 scalpel. Tissue samples were lyophilized overnight and then weighed (dry weight). Constructs were then digested by papain (80 μg/mL) and stored at -20°C until analysis. Aliquots of the digest were assayed separately for proteoglycan, collagen and DNA contents. The proteoglycan content was estimated by quantifying the amount of sulphated glycosaminoglycans using the dimethylmethylene blue dye binding assay[107,108]. Collagen content was estimated from the determination of the hydroxyproline content. Aliquots of the papain digest were hydrolyzed in 6 N HCl at 110ºC for 18 hours and the hydroxyproline content of the hydrolyzate was then determined using chloramine-T/Ehrlich's reagent assay[109]. Collagen content was estimated assuming hydroxyproline accounts for 10% of the total collagen mass in cartilage[110]. The DNA content was estimated using the Hoechst 33258 dye assay[101]. Similarly, the remaining portion of the implanted construct was saved after surgery (stored at -20°C) and analyzed to assess biochemical remodeling during implantation.

### 4.3.5 Histological and immunohistochemical evaluation.

For histological/immunohistochemical evaluation, the remaining half of the defect site (implant and surrounding native tissue) and the underlying bone was removed. Sample were fixed with 4% paraformaldehyde (w/v) over 72 hours and decalcified in 10% EDTA (w/v) (pH 6.5, Sigma-Aldrich) over a 5 week period at room temperature on an orbital shaker with solutions changed twice per week. Decalcified tissue samples were embedded in paraffin and thin sections (5 μM) were cut. Sections were stained with either Weigert's Iron hemotoxylin-eosin (H&E, a general connective tissue stain) and Masson's Trichrome (to stain collagen). After staining, sections were dehydrated by sequential immersion in alcohol, mounted with mounting medium, and examined by light microscopy. Additional sections were cut, sent to the University of Guelph (Dr. Mark Hurtig, Clinical Studies) where they were stained with safranin-O and scored using the ICRS II Histological Scoring system[142,143] (Appendix B, Table B1) to assess the extent of integration and healing. ICRS II scoring was performed blinded by Dr. Mark Hurtig.

Sections for immunohistochemical staining were immersed in 3% $H_2O_2$ (v/v) for 10 minutes to quench endogenous peroxidase activity[112]. To reduce non-specific protein binding, the sections were blocked with horse serum (Vector Laboratories Inc., Burlingame, CA, USA), in PBS (pH 7.4) for 30 minutes at room temperature. Type I collagen sections were incubated with mouse monoclonal type I primary antibody (I-8H5: Daiichi Fine Chemicals Co Ltd, Japan) at 40 μg/mL in 10% serum (v/v) in PBS (pH

7.4) overnight at 4°C. Type II collagen sections were incubated with mouse monoclonal type II primary antibody (II-II6B3: Developmental Studies Hybridoma Bank, University of Iowa, IA, USA) at a 1:200 dilution in 10% horse serum (v/v) in PBS (pH 7.4) overnight at 4°C. Following primary antibody incubation, sections were rinsed in PBS (pH 7.4), and incubated with biotinylated secondary antibodies using the Vectastain® Elite ABC kit (Vector Laboratories) with 10% horse serum (v/v) in PBS. Immunodetection was performed using 3, 3'-diaminobenzidine tablets (Sigma-Aldrich) for colour development according the ABC kit instructions. Sections were counterstained with nuclear fast red stain for 10 seconds. Sections were then cleared and mounted with mounting medium and examined by light microscopy. To assess non-specific staining, the primary antibody was omitted from each type of section.

### 4.3.6 Statistical analyses.

All results were expressed as the mean ± standard error of the mean (SEM). Collected data was analyzed statistically using either a one-way or two-way analysis of variance (ANOVA) and the Fisher's least significant difference (LSD) post-hoc test. Data was checked prior to performing statistical tests for both normality and equal-variance. Macroscopic scoring results were analyzed using the non-parametric Krusal-Wallis test. All statistical tests were conducted using statistical software (SPSS version 16, SPSS Inc., Chicago, IL, USA). Significance was associated with p-values less than 0.05 and trends were noted with p-values between 0.05 and 0.1.

## 4.4 Results and Discussion

### 4.4.1 Evaluation of post-operative healing.

All of the animals used for this study recovered from the operation. By the end of a week all but one rabbit exhibited a full recovery (data not shown). This rabbit experienced a displaced patella and had to undergo corrective surgery. After the second surgery, the rabbit made a full recovery and was kept in the study. Prior to euthanasia, all of the animals at each time point had completely healed scars and exhibited normal behaviour and gait, with no discernable differences between animals of different time groups or controls.

### 4.4.2 Macroscopic evaluation of retrieved implants.

As early as one month post-implantation, 83% of the grafts were smooth and level with the surrounding native cartilage and had complete integration, receiving nearly perfect scoring (Figure 4-1 and Table 4-1). After 3 months implantation, 33% of the grafts received perfect scoring and the remaining 67% received nearly normal scoring. At 6 months, 67% of the grafts were characterized with smooth surfaces and good integration, receiving perfect scoring and 33% received nearly normal scoring. At each time point, the colour of the implanted tissue varied from yellow to a semi translucent white, similar to that of native cartilage. Out of the 18 rabbits, all but two of the defects received an ICRS score higher than 8, corresponding to a normal or nearly normal over-all repair assessment. There was no significant difference observed in ICRS scoring of the treated

animals at any time points. In all cases, the surrounding cartilage was intact and displayed no apparent signs of degeneration.

In contrast to the uniform appearance of treated defects at each time point, macroscopic examination of the control defects displayed varying degrees of tissue resurfacing (Figure 4-1 and Table 4-1). Control repair tissue at 1 and 3 months was white in appearance with limited filling of the defect site (~50%) and poor integration with surrounding native cartilage. At 6 months, the control defect site had more repair tissue but was still characterized by a fibrillated surface.

**Table 4-1 Macroscopic ICRS score for the defects at 1, 3 and 6 months as well as control groups.** Data was pooled and presented as mean rank (*n = 6* samples/group for treated defects). Statistical analyses were not performed for the control groups.

| | **Categories** | | | **Total score (out of 12)** |
|---|---|---|---|---|
| | **I (out of 4)** | **II (out of 4)** | **III (out of 4)** | |
| **1 Month** (*n=6*) | 3.3 | 3.5 | 3.5 | 10.3 |
| **3 Months** (*n=6*) | 3.2 | 3.5 | 3.7 | 10.3 |
| **6 Months** (*n=6*) | 3.8 | 4 | 3.8 | 11.7 |
| **Control 1 Month** (*n=2*) | 2 | 1 | 1 | 4 |
| **Control 3 Months** (*n=2*) | 1.5 | 1 | 1.5 | 4 |
| **Control 6 Months** (*n=1*) | 2 | 2 | 2 | 6 |
| **Categories:** *I*: Degree of Defect Repair, *II*: Integration to Border Zone, and *III*: Macroscopic Appearance | | | | |

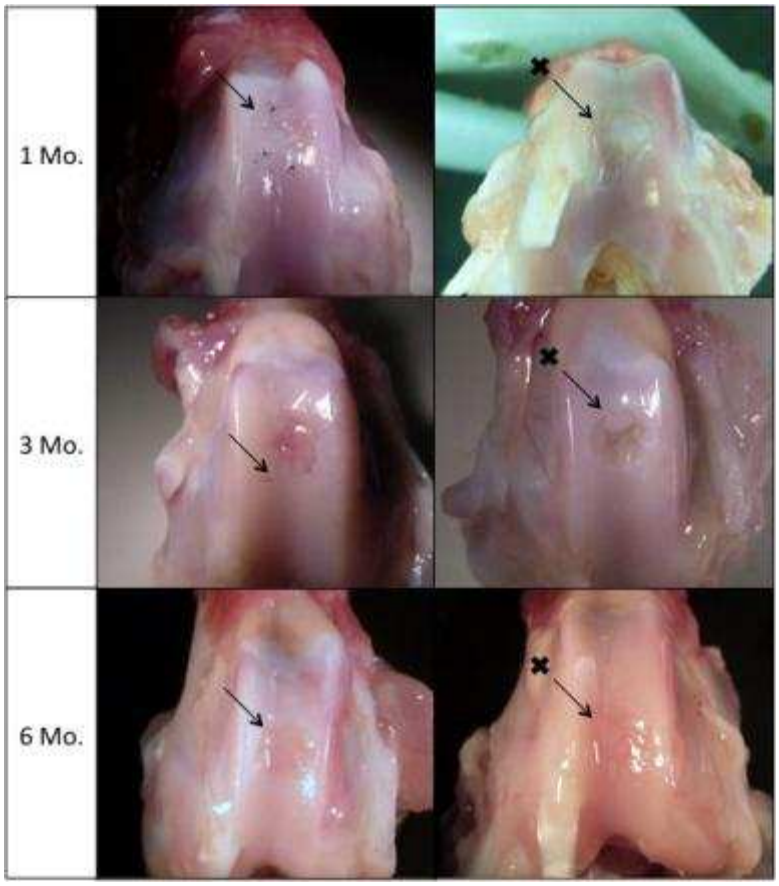


**Figure 4-1 Effect of increasing implant time on repair response**. Macroscopic appearance of the treated defects (left) and control defects (right) at 1, 3 and 6 months.

### 4.4.3 Histological and Immunohistichemical evaluation of retrieved implants.

Loss of the implanted graft was not a significant problem and intact, implanted constructs were observed in over 70% of the animals (Figure 4-2). Three out of the thirteen intact defects had a small layer of fibrous tissue on top of the implant. Discrepancies observed within repair responses of different defects can be attributed to a variety of factors. For example, variability can occur within the animals used, in addition to biochemical and

morphological differences between the pre-implanted constructs used for the surgeries[25,129]. Nonetheless, at all time points, repair tissue stained positively for collagen type II and had little to no collagen type I staining (Figure 4-3) (Appendix D, Figure D1, D2 and D3). Between treated and control defects, total histological scores increased at both 1 and 3 month time points. At all time points, the repair tissue in the treated defects was ~50% hyaline cartilage (Table 4-2). When using allogenic cells to generate the constructs, there is always the possibility of immunological responses[25]. Histological grading revealed that there was inflammation present in the treated defects at each time point. However the presence of inflammation was also mirrored in the control defects and may have been caused by the deposition of fibrin glue within the defect.

Critical to the survival of an implanted graft is a close contact with the surrounding cartilage[130]. To achieve this close fit, there must be adequate anchoring of the implant within the defect. In an effort to address this issue, a number of fixation techniques have been currently used with *in vivo* implantation studies. Commonly used construct fixation methods include: press fitting, sutures, fibrin glue, or a mixture of all three[40]. As these techniques can affect the repair response, optimal retention of the grafts should be achieved through minimal fixation. Implant fixation is also largely dependent on the defect type. While press-fit fixation alone is sufficient for osteochondral transfer, additional fixation methods are typically required for chondral repair[82] as previous studies have shown high rates of implant loosening during the repair of chondral

defects[9,82]. A combination of fibrin glue with sutures is a popular technique employed in many animal defect models[81,130,131]. In the present study, fibrin glue and sutures were used not only to help secure the implant into the defect site but to merge the perimeter of the construct to the adjacent cartilage. Masson's trichrome staining of the treated defects indicated integration of the implant with surrounding native cartilage and good fixation to the underlying subchondral bone. Upon close examination at 6 months (Figure 4-3), the junction between the implant and the surrounding native cartilage was nearly indistinguishable. The use of the fibrin glue helps not only in the retention of the constructs but also serves to fill resulting gaps between the implant and adjacent cartilage and increase integration the potential of the implanted constructs. Poor integration of the implant is also a commonly encountered problem, which can be exacerbated by the fact that the chondrocytes do not tend to migrate towards, or from, the construct[82,126]. In addition, gaps present during the repair of chondral defects are isolated from spontaneous repair and do not necessarily fill with fibrocartilage tissue and such poorly integrated surfaces are not well suited to withstand mechanical forces within the joint[5,9]. The tight contact achieved in the present study between the implanted construct and adjacent cartilage was encouraged with the use of fibrin glue and sutures led to the nearly indistinguishable junctions observed at 6 months post-operatively.

The filling of control defects appeared to be random and the resulting repair tissue was mostly disorganized and fibrous in nature (Figure 4-2). Limited coverage of control

defects was evidenced in all 1 month and 3 month post-operative defects. Integration between the control repair tissue and subchondral bone at these time points was also absent. Surprisingly, the repair response exhibited at six months enabled complete coverage of the entire defect area in line with the adjacent native cartilage. However, the cartilage thickness in this defect was less than half that of original cartilage thickness and was mainly filled with subchondral bone. Although spontaneous repair of purely chondral defects does not typically occur[82,122], several factors could explain the occurrence of repair tissue in the control defects. When the defects were established, care was taken not to disrupt the underlying subchondral but there were trace amounts of blood present at the defect sites. The application of fibrin glue may have trapped the blood within the site, influencing the repair response. The presence of blood in a defect site will initiate a spontaneous repair response[9]. Alternatively, several studies have shown the contribution of the phenomenon known as "matrix flow" to cartilage repair[132,133,134]. This mechanism involves the migration of the adjacent cartilage towards the defect site. Closer observation of the native cartilage at the periphery of the defect site, especially at 1 and 3 months post-operatively (Figure 4-3), revealed the presence of rounded tissue, falling towards the empty (untreated) defect. At six months, the untreated defect site was covered with a thin hyaline-like tissue (~ 20% of the thickness of the surrounding native cartilage), exhibiting predominantly type II collagen staining. This result was consistent with other studies that have observed type II collagen in control repair tissue for up to one year after defect creation[135,136]. Although little is known about matrix flow and its

contribution to defect repair, many agree that the resulting repair tissue is inferior to that of normal hyaline cartilage and is susceptible to further degeneration[132,133]. Of more concern was the observed inflammation (Table 4-2) and the thickening of the underlying subchondral bone (Figure 4-2). Although histological grading did not find abnormalities in the subchondral bone of the 6 months control, it rises into over half of the cartilage thickness. Subchondral bone thickening is typically associated with early stage osteoarthritis. The increased bone volume at the subchondral bone surface occurs as with decreasing bone density at this location[26,137]. It is possible that the repair tissue within these untreated (control) defects will eventual degenerate leading to the onset of osteoarthritic joint disease.

Hyaline-like architectural organization of the implants was observed at each time point. Initially, the implanted constructs were hyper-cellularized in comparison to native articular. However, the construct's DNA content approached the levels of the surrounding cartilage with increasing implantation time. Zonal stratification, essential determinant of articular cartilage's mechanical properties[1], was demonstrated as early as 1 month post-implantation. The presence of a columnar arrangement of cells in the deeper zones accompanied with flattened cells at surface of the implant (Figure 4-4) was suggestive of a structural reorganization of the implants towards that of native cartilage after implantation[1,24].

**Table 4-2 Histological scoring at 1, 3 and 6 months as well as control groups[142,143].** Total score presented as mean ± SEM. No significant differences for the total score were found between the treated groups.

| | Categories (out of 100) | | | | | | | | | | | | | | Total (out of 1400) |
|---|---|---|---|---|---|---|---|---|---|---|---|---|---|---|---|
| | **I** | **II** | **III** | **IV** | **V** | **VI** | **VII** | **VIII** | **IX** | **X** | **XI** | **XII** | **XIII** | **XIV** | |
| **1 Month (*n=6*)** | 58 | 52 | 42 | 18 | 51 | 67 | 3 | 41 | 43 | 90 | 48 | 32 | 39 | 43 | 626 ± 127 |
| **3 Month (*n=6*)** | 44 | 44 | 46 | 43 | 44 | 49 | 0 | 66 | 70 | 79 | 70 | 43 | 44 | 44 | 687 ± 142 |
| **6 Month (*n=6*)** | 48 | 50 | 50 | 40 | 40 | 65 | 0 | 50 | 48 | 75 | 79 | 40 | 62 | 53 | 701 ± 81 |
| **1 Month Control (*n=2*)** | 15 | 30 | 33 | 45 | 10 | 20 | 0 | 25 | 40 | 60 | 45 | 13 | 28 | 25 | 388 ± 148 |
| **3 Month Control (*n=2*)** | 8 | 8 | 10 | 13 | 5 | 5 | 0 | 38 | 35 | 85 | 55 | 0 | 8 | 8 | 275 ± 80 |
| **6 Month Control (*n=1*)** | 30 | 30 | 35 | 20 | 25 | 80 | 0 | 80 | 85 | 90 | 90 | 20 | 60 | 55 | 700 |

**Categories:** I: Tissue Morphology, II: Matrix staining, III: Cell morphology, IV: Chondrocyte clustering, V: Surface architecture, VI: Basal integration, VII: Tidemark formation, VIII: Subchondral bone abnormality, IX: Inflammation, X: Abnormal calcification, XI: Vascularization, XII: Superficial zone, XIII: Mid/deep zone and XIV: Overall assessment

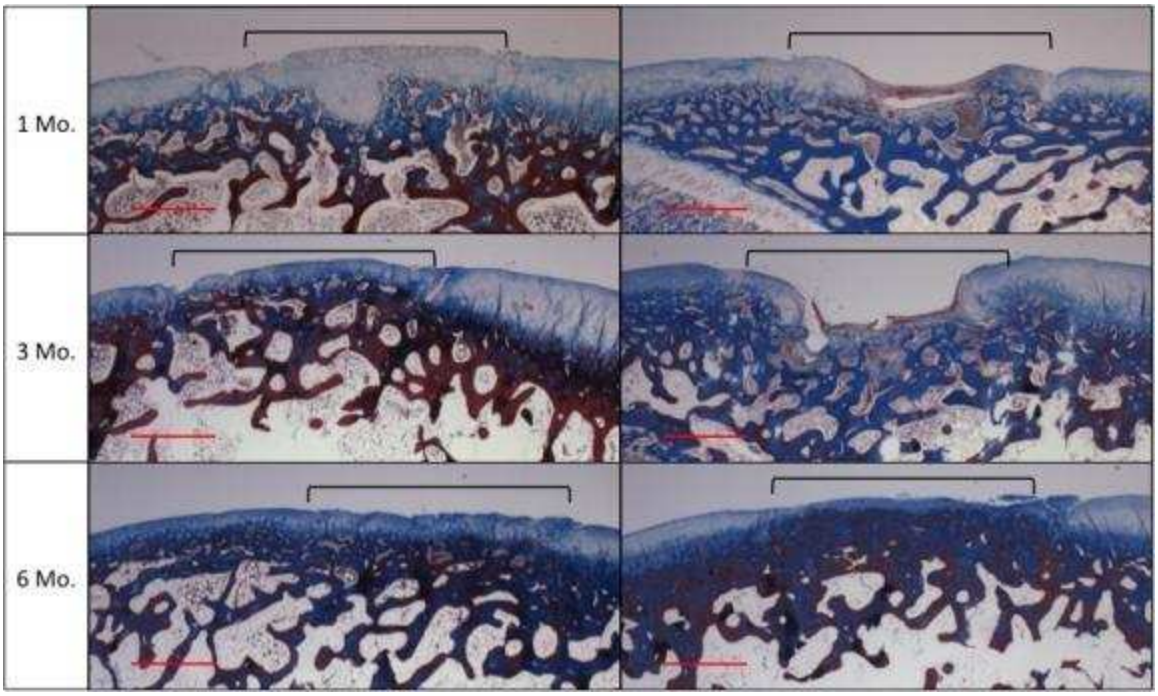


**Figure 4-2 Extent of defect filling with repair tissue at each time point**. Masson's trichrome staining of the treated defects (left) and control defects (right) at 1, 3 and 6 months post-operatively. Defect area is outlined in black (scale bar: 100 μm).

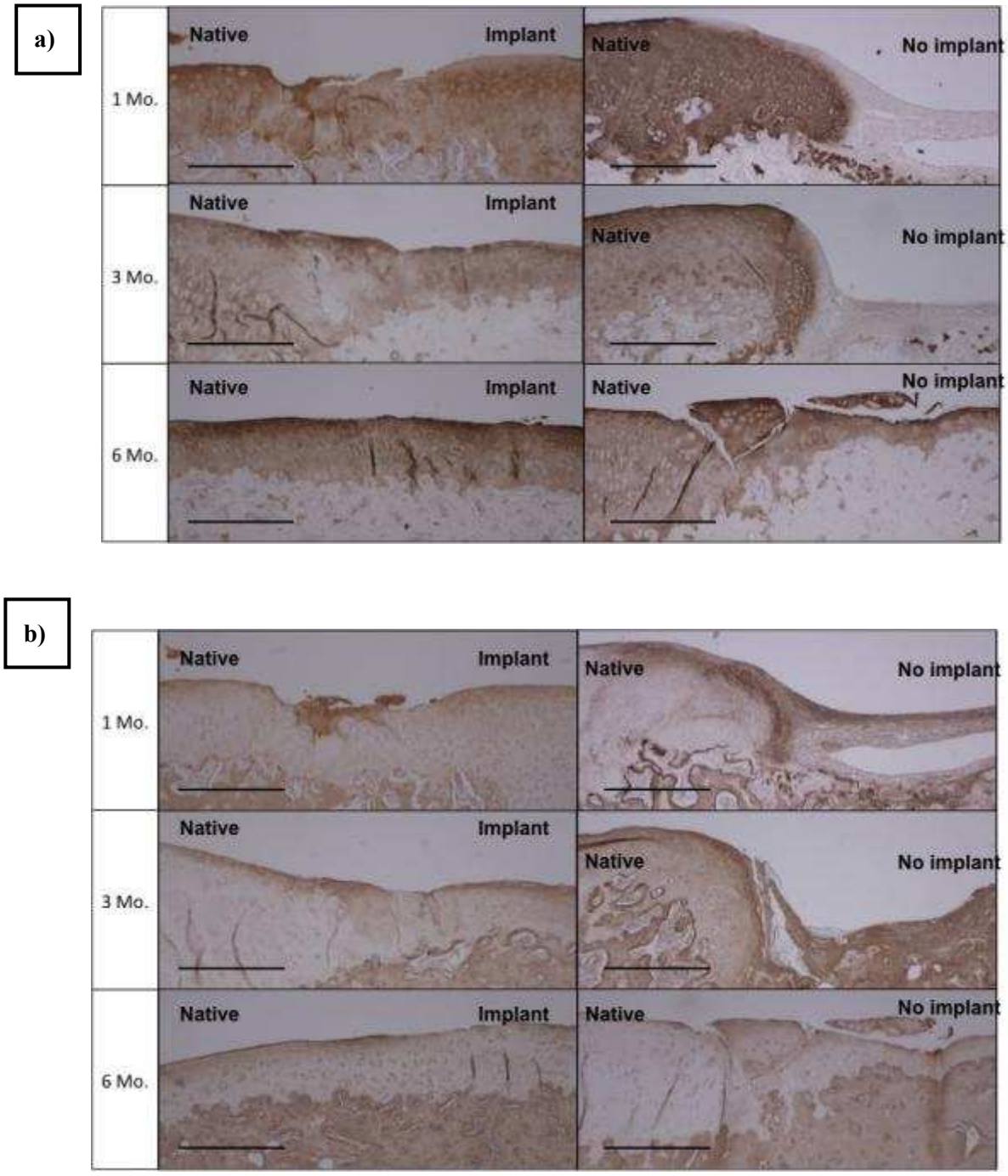


**Figure 4-3 Effect of implant time on integration and presence of cartilage biomarkers**. Immunohistochemical staining treated defects (left) and control defects (right) at 1, 3 and 6 months post-operatively. (A) Type II collagen staining of the implant and control knee (B) Type I collagen staining of the implant and control knee (scale bar: 500 μm)

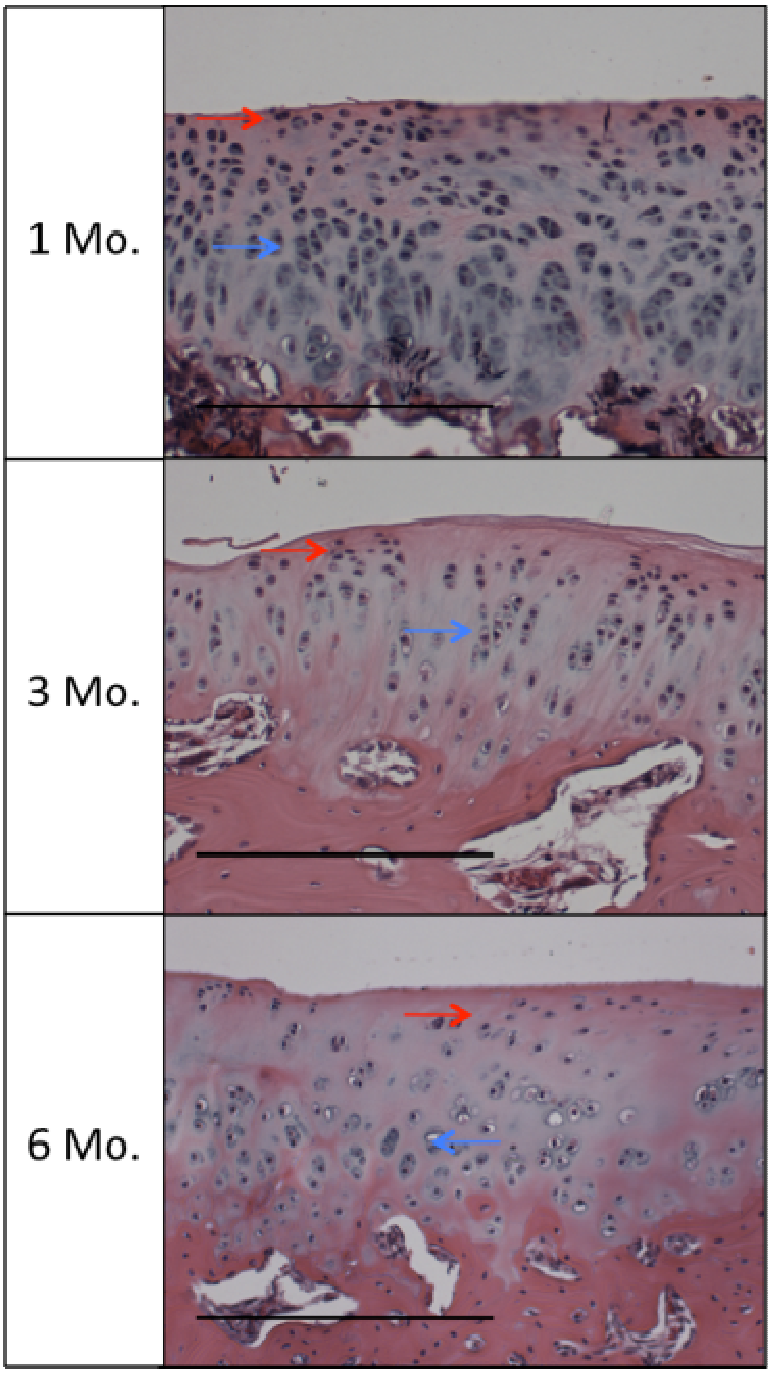


**Figure 4-4 Effect of implant time on morphological appearance on repair tissue**. Architectural organization of the implant at 1, 3 and 6 months post-operatively, red arrows indicate flattened surface cells and blue arrows indicate columnar formation of deeper zone chondrocytes (H&E stain, scale bar: 300 μm)

### 4.4.4 Biochemical evaluation of retrieved constructs.

Biochemical properties of the implanted cartilage were evaluated to determine the extent of matrix remodeling after implantation (Table 4-3). Post-operatively, the biochemical constituents of the implants decreased with increasing implantation time. However, the same trend was also observed in the surrounding native cartilage with increasing animal age. Measured collagen-to-proteoglycan levels were not significantly different from one another or between native cartilage and implants. As observed histologically, beyond 1 month post-operatively, there was a significant decrease in DNA content within the implant. Tissue cellularity at the later time points was similar to the level of native cartilage. Proteoglycan content of the pre-implanted constructs was higher than native cartilage but decreased with longer implantation times. Conversely, collagen levels between the pre- and post-implanted constructs initially increased by >50% upon implantation. The decrease in proteoglycan levels and collagen with increasing implantation time was also observed in the surrounding native cartilage with increasing animal age. Although proteoglycan and collagen levels were lower than that of native cartilage, the collagen-to-proteoglycan ratio of the implant was comparable to the adjacent cartilage.

Upon implantation, the highly controlled *in vitro* culture is replaced with the dynamic environment of the knee. The survival of the constructs demonstrated that they were able to support the imposed mechanical forces of the joint. As mechanical stimulation is

intimately linked with chondrocyte behavior and ECM maintenance, it was reasoned that these biological forces encouraged remodeling of the constructs towards the structure and composition of native cartilage[5,138]. In addition to exposure to mechanical joint forces, the implanted constructs were also exposed to signaling molecules present in the joint. As seen with mechanical loading of the tissue, released signaling molecules can have a stimulatory effect on cartilage tissue growth[56]. Growth factors including IGF, FGF and PDGF are involved with the mediation of chondrogenic physiology. Studies have shown enhanced ECM expression and histological organization of engineered constructs with the addition of IGF-1 with bFGF and TGF-β2[56,139]. As such, the exogenous factors present in the knee not only maintained the constructs for up to 6 months, they also encouraged the remodeling of the repair tissue into a hyaline-like cartilage.

**Table 4-3** Biochemical evaluation properties of implants at 1, 3 and 6 months. Results from each time point were pooled, and data presented as mean ± SEM (*n* = 6 samples/group)

| | | **DNA [µg/mg]** | **PG [µg/mg]** | **Col [µg/mg]** | **Col:PG** |
|---|---|---|---|---|---|
| **1 Month (n=6)** | Native | 3.9 ± 0.5 | 172 ± 17† | 380 ± 70† | 2.7 ± 0.2 |
| | Implant | 7 ± 1* | 122 ± 24 | 234 ± 55 | 2.8 ± 0.6 |
| **3 Months (n=6)** | Native | 2.7 ± 0.5 | 143 ± 23† | 465 ± 49† | 3.4 ± 0.3 |
| | Implant | 2.2 ± 0.4 | 93 ± 25 | 214 ± 68 | 3 ± 1 |
| **6 Months (n=6)** | Native | 2.7 ± 0.5 | 116 ± 21† | 351 ± 58† | 3.5 ± 0.8 |
| | Implant | 2.7 ± 0.5 | 60 ± 10 | 208 ± 54 | 4 ± 1 |
| **Original Construct (n=6)** | | 2.3 ± 0.3 | 238 ± 31 | 122 ± 8 | 0.6 ± 0.1 |

Results normalized to tissue dry weight; PG: proteoglycans; Col: collagen
* different from other time points ($p<0.01$); † difference between implant/native ($p<0.01$)

## 4.5 Conclusion

In this study, it was shown that scaffold-free engineered constructs developed from a relatively small population of cells can survive full weight bearing and repair critical sized chondral defects. The method of implant fixation was sufficient, with implants losses occurring in ~30% of the defects, as other studies have reported implant loosening within chondral defects in up to 55% of the defects[82]. Additionally, the implanted tissues appeared to remodel, both structurally and biochemically, towards that of native cartilage with increasing time *in vivo*. In comparison with control defects, the repair tissue in the treated defects was both histologically and morphologically superior.

The utility of this approach is that either an allogenic or autogenic based repair strategy can be employed. In this study, the feasibility of using allogenic cells has been demonstrated for effective cartilage repair with minimally observed immunological implications. This may be an attractive approach if the availability of autogenic cells are limited. Alternatively, an autogenic based approach is also a viable option. The small amount of cells required for this approach circumvents two major drawbacks of common surgical techniques: i) donor-site morbidity and ii) availability donor tissue[9,82]. Results from this animal study demonstrate that the engineered implants may offer an effective treatment option as constructs can be generated from a small patient cartilage biopsy and adopt an articular cartilage-like appearance post-implantation. These initial results are promising and warrant further investigation to determine their full repair potential. As

healing success rates have been shown to be influenced with animal age[40,79], these results need to be repeated in an older animal model. Other considerations include the location of the defect in the knee joint. Success rates of other surgical interventions have been shown to rely heavily on the defect location[40]. The patellofemoral groove (or trochlea) has been described as a low-weight bearing region and was an obvious choice to test newly developed tissue engineered constructs[77]. Future studies will include construct fixation in the more demanding mechanical environments, such as the femoral condyle.

# Chapter 5

# Conclusions and Recommendations

## 5.1 Overall Perspective

The use of cartilage resurfacing techniques, including mosaic arthroplasty and ACT, has generally been successful in short-term clinical applications. Although these procedures have resulted in good healing outcomes of articular defects, the absence of long-term clinical trials to identify potential unfavorable side effects is of concern. The common practice of these techniques in a clinical setting has failed to adequately address various short-comings in these methods. This includes the limitation associated with extraction of donor tissue that is required for these techniques. Donor site morbidity occurs in mosaic arthroplasty, as the osteochondral plugs are harvested from otherwise undisturbed regions of the joint. Isolated chondrocytes, used in ACI, require biopsies extracted from the healthy tissue. While expansion of these cells *in vitro* can adequately increase cell number, it is also associated with de-differenciation and loss of potency[20].

Another limitation encountered with these techniques involves the securing of the graft or cells within the defect site. Loss of the periosteal flap, whose main role is to trap the isolated chondrocytes within the defect, is not uncommon with ACI[9]. With mosaic arthroplasty, the issue is not in the loss of osteochondral plugs, but rather with graft fixation and stability. Multiple plugs are secured within the defect to maximize filling of

the void, resulting in the formation of interstices between adjacent grafts. Fibrocartilage will fill in these spaces, compromising the ability of the grafts to integrate with surrounding native cartilage. Without proper integration, interfaces between repair tissue and native cartilage are not well suited to withstand mechanical forces within the joint[5].

In an attempt to circumvent limitations associated with previous resurfacing techniques, this has described an approach to generate large-sized engineered constructs ($\geq 3$ $cm^2$) directly from a small number of cells. The first objective was to determine optimal growing conditions for the constructs and to illustrate limited chondrocyte de-differentiation, even in the absence of a scaffold. The second objective was to evaluate integrative potential and the reparative nature of the constructs implanted in a rabbit defect model.

### 5.1.1 *In vitro* culture

From this investigation, it has been demonstrated that the continuous flow bioreactor culture required only a small amount of cells encouraged chondrogenic phenotype and the development of a hyaline-like tissue. The amount of cells required for culture was 20 times less that of ACI and the resulting construct was $3cm^2$ (clinically-relevant defects: 1.5 - $6.5cm^2$). The development of zonal differences throughout tissue depth is indicative of tissue remodeling. As early as 3 weeks, these constructs exhibited tissue remodeling in both histological and biochemical assessment.

In comparison to native articular cartilage, the engineered constructs were similar in terms of thickness, proteglycan content and displayed homogenous distribution of collagen type II. At 3 weeks culture time, changes in construct composition appeared to level off and this was the culture period chosen for the implantation study. Accumulation of collagen and resultant mechanical properties were inferior to that of native cartilage. However, increases in culture time to mature the constructs might limit their potential to integrate with the defect site and surrounding cartilage, which is crucial for long-term graft survival[9,23].

### 5.1.2 *In vivo* culture

Even with inferior mechanical properties and collagen content, the engineered constructs were able to survive in full weight bearing. Upon implantation, the generated tissue constructs were able to adopt both the structure and biochemical composition similar to that of native cartilage. Remodeling of the construct towards a hyaline-like tissue, was seen at every time point (1, 3 and 6 months) post-operatively. Macroscopically, the surface of the implanted constructs was in line with the native cartilage and there appeared to be a close fit between the two. Histological examination of the implanted constructs revealed little to no gaps in the junctions and good integration with the subchondral bone. By six months post-operatively, some of the implant junctions were indistinguishable from that of native cartilage.

## 5.2 Recommendations

When left untreated, chondral defects have the potential to initiate degenerative osteoarthritis[140]. The aim of cartilage resurfacing techniques is to fill these defects with a hyaline-like tissue in order to prevent this unfavorable outcome. The engineered constructs developed in this study from a small amount of cells, have demonstrated their effectiveness in the short-term repair of chondral defects. In addition, a number of limitations, previously encountered with other resurfacing techniques, have been avoided through this novel culture method and with proper fixation of the constructs within the defect. It is important to note that this technique is aimed at purely chondral defects, as these implants do not possess a bony component.

One question that must be addressed is whether the repair capacity of the engineered constructs has long-term therapeutic potential. The 6-month follow-up period of the constructs has been shown by other studies to be a reasonable amount of time for first evaluations[78]. However, with the generation of satisfactory results, this follow-up period should be extended for long-term evaluation of the construct's *in vivo* performance. Additionally, when considering the mechanical environment of the joint, the femoral patellar groove is thought of as non-weight bearing. Defect location can influence the repair response, as seen with other resurfacing techniques[9]. Future studies could include construct implantation in higher load bearing zones, such as the femoral condyle, to assess the mechanical integrity of the constructs.

Mechanical properties and collagen contents of the engineered constructs were significantly inferior to that of native cartilage. As such, more work should be carried out to mature the constructs *in vitro* if implant location is to be evaluated in the femoral condyle. Incorporation of various signaling molecules with cell culture has been investigated for their influence on the chondrocyte and promotion of tissue growth. Growth factors, including TGF-β, FGF and IGF, have been shown to increase expression of hyaline ECM[56]. Other signaling molecules, such as ATP supplementation[141], have exhibited dose-dependent effects on chondrocyte behaviour and ECM composition. Further investigations of the influence of signaling molecules on the engineered constructs from this study may help to improve their mechanical properties. However, beneficial changes to the construct's properties must not compromise the integrative potential of the implants. Signaling molecules, in conjunction with this culture method could also allow for the use of older chondrocytes. The diminished proliferative and synthesizing capacities associated with aged chondrocytes could be avoided with the correct signaling molecule(s). Individuals requiring cartilage repair has been correlated with increasing age, thus limiting the availability of young chondrocytes for harvest. Optimizing this culture method with future clinical applications in mind will not only produce a superior construct but will hopefully aid in its clinical translation.

# References


(1) Poole, A.; Kojima, T.; Yasuda, T.; Mwale, F.; Kobayashi, M.; Laverty, S. *Clinical Orthopaedics and Related Research* **2001**, *391*, S26.

(2) Haasper, C.; Zeichen, J.; Meister, R.; Krettek, C.; Jagodzinski, M. *Injury* **2008**, *39*, 66–76.

(3) Buckwalter, J.; Mankin, H. *The Journal of Bone and Joint Surgery* **1997**, *79*, 600.

(4) Wieland, H. A.; Michaelis, M.; Kirschbaum, B. J.; Rudolphi, K. A. *Nat Rev Drug Discov* **2005**, *4*, 331–344.

(5) Temenoff, J.; Mikos, A. *Biomaterials* **2000**, *21*, 431–440.

(6) Lee, C.; Grad, S.; Wimmer, M. *Topics in tissue engineering* **2005**.

(7) Buckwalter, J. *Clinical Orthopaedics and Related Research* **2002**, *402*, 21.

(8) Mano, J.; Reis, R. *Journal of Tissue Engineering Regenerative Medicine* **2007**, *1*, 261–273.

(9) Hunziker, E. *Osteoarthritis and Cartilage* **2002**, *10*, 432–463.

(10) Buckwalter, J. A.; Mow, V. C.; Ratcliffe, A. *Journal of the American Academy of Orthopaedic Surgeons* **1994**, *2*, 192–201.

(11) Jackson, D.; Simon, T.; Aberman, H. *Clinical Orthopaedics and Related Research* **2001**, *391*, S14.

(12) Nesic, D.; Whiteside, R.; Brittberg, M.; Wendt, D.; Martin, I.; Mainil-Varlet, P. *Advanced Drug Delivery Reviews* **2006**, *58*, 300–322.

(13) Brittberg, M.; Lindahl, A.; Nilsson, A.; Ohlsson, C. *New England Journal of Medicine* **1994**, *331*, 889–895.

(14) Hangody, L.; Kish, G.; Karpati, Z.; Udvarhelyi, I.; Szigeti, I. *Orthopedics* **1998**.

(15) Gilbert, J. *American Journal of Knee Surgery* **1998**, *11*, 42–46.

(16) Breinan, H.; Minas, T.; Hsu, H.; Nehrer, S.; Sledge, C.; Spector, M. *JBJS* **1997**, *79*, 1439–51.

(17) Horas, U.; Pelinkovic, D.; Herr, G.; Aigner, T.; Schnettier, R. *The Journal of Bone and Joint surgery* **2003**, *85*, 185–192.

(18) Solchaga, L.; Goldberg, V.; Caplan, A. *Clinical Orthopaedics and Related Research* **2001**, *391*, S161.

(19) Hunziker, E. *Osteoarthritis and Cartilage* **2001**, *10*, 432–463.

(20) Darling, E.; Athanasiou, A. *Journal of Orthopaedic Research* **2005**, *23*, 425–432.

(21) Laurencin, C. T.; Ambrosio, A.; Borden, M. D.; Cooper, J. A. *Tissue engineering: Orthopedic Applications* **1999**, *1,* 19-46

(22) Darling, E.; Athanasiou, A. *Tissue Engineering* **2005**, *11*, 395–403.

(23) Klein, T. J.; Malda, J.; Sah, R. L.; Hutmacher, D. W. *Tissue Engineering Part B: Reviews* **2009**, *15*, 143–157.

(24) Hayes, A.; Hall, A.; Brown, L.; Tubo, R.; Caterson, B. *Journal of Histochemistry & Cytochemistry* **2007**, *55*, 853–866.

(25) Revell, C.; Athanasiou, K. *Tissue Engineering Part B: Reviews* **2008**, *15*, 1–15.

(26) Ulrich-Vinther, M.; Maloney, M.; Schwarz, E.; Rosier, R.; O'keefe, R. *Journal of the American Academy of Orthopaedic Surgeons* **2003**, *11*, 421–430.

(27) Huber, M.; Trattnig, S.; Lintner, F. *Investigative radiology* **2000**, *35*, 573.

(28) Buckwalter, J.; Einhorn, T.; Simon, S. *Orthopaedic Basic Science Biology and Biomechanics of the Musculoskeletal System*; American Academy of Orthopaedic

Surgeons: Rosemont, Il, **2000**.
(29) Netter, F. *Atlas of Human Anatomy*. East Hanover: Novartis, **1999**.
(30) Stockwell, R. *Journal of Anatomy* **1967**, *101*, 753–763.
(31) Mithoefer, K.; Williams, R. J.; Warren, R. F.; Wickiewicz, T. L.; Marx, R. G. *American Journal of Sports Medecine* **2006**, *34*, 1413-1418
(32) Meachim, G. *Clinical Orthopaedics and Related Research* **2001**, *391S*, S6-S13.
(33) Stoddart, M. J.; Grad, S.; Eglin, D.; Alini, M. *Regenerative Medicine* **2009**, *4*, 81–98.
(34) Schulz, R.; Bader, A. *European Biophysics Journal* **2007**, *36*, 539–568.
(35) Poole, C. *Journal of Anatomy* **1997**, *191*, 1–13.
(36) Cohen, N. P.; Foster, R. J.; Mow, V. C. *Journal of Orthopaedic & Sports Physical Therapy* **1998**, *28*, 203–203.
(37) Mauck, R.; Suscheck, C. V. *Engineering Cartilage Tissue*; From Lab to Clinic; 1st ed. Tissue Engineering: From Lab to Clinic: Berlin, Germany, **2011**, 634.
(38) Hunziker, E. *Clinical Orthopaedics and Related Research* **1999**, *367*, S135-S146.
(39) Chiang, H.; Jiang, C. *Journal of the Formosan Medical Association* **2009**, *108*, 87-101.
(40) Reinholz, G. G.; Lu, L.; Saris, D. B. F.; Yaszemski, M. J.; O'Driscoll, S. W. *Biomaterials* **2004**, *25*, 1511–1521.
(41) Steadman, J.; Briggs, K.; Rodrigo, J. *The Journal of Arthroscopic and Related Surgery* **2003**, *19*, 477–484.
(42) Bhosale, A. M.; Richardson, J. B. *British Medical Bulletin* **2008**, *87*, 77–95.
(43) Redman, S.; Oldfield, S. *European Cells and Materials* **2005**, *9*, 23–32.
(44) Minas, T. *Clinical Orthopaedics and Related Research* **2001,** *391S*, S349-S361.
(45) Peterson, L.; Minas, T.; Brittberg, M.; Nilsson, A.; Sjogren-Jansson, A.; Lindahl, A. *Clinical Orthopaedics and Related Research* **2000**, *374*, 212–234.
(46) Peterson, L.; Brittberg, M.; Kiviranta, I.; Lundgren, E.; Lindahl, A. *American Journal of Sports Medicine* **2002**, *30*, 2–12.
(47) Roberts, S.; McCall, I.; Darby, A.; Menage, J.; Evans, H.; Harrison, P.; Richardson, J. *Arthritis Research and Therapy* **2003**, *5*, R60–R73.
(48) Smith, G.; Knutsen, G.; Richardson, J. *The Journal of Bone and Joint Surgery-British Edition* **2005**, *87-B*, 445–449.
(49) Ruanoravina, A.; Jatodiaz, M. *Osteoarthritis and Cartilage* **2006**, *14*, 47–51.
(50) Matsusue, Y.; Yamamuro, T.; Hama, H. *Arthroscopy: The Journal of Arthroscopic and Related Surgery* **1993**, *9*, 318–321.
(51) Wei, X.; Gao, J.; Messner, K. *Journal of Biomedical Materials Research Part A* **1997**, *34*, 63–72.
(52) Hangody, L.; Feczkó, P.; Bartha, L.; Bodo, G.; Kish, G. *Clinical Orthopaedics and Related Research* **2001**, *391S*, S328–S336.
(53) Laprell, H. *Archives of Orthopaedic and Trauma Surgery* **2001**, *121*, 248-253.
(54) Bentley, G.; Biant, L. C.; Carrington, R. W. J.; Akmal, M.; Goldberg, A.; Williams, A. M.; Skinner, J. A.; Pringle, J. *The Journal of Bone and Joint Surgery* **2003**, *85*, 223–230.
(55) Iwasaki, N.; Kato, H.; Kamishima, T.; Suenaga, N.; Minami, A. *American journal of Sports Medecine* **2007**, *35*, 2096-2100.
(56) Kuo, C.; Li, W.; Mauck, R.; Tuan, R. *Current opinion in rheumatology* **2006**, *18*,

64-73.
(57) Chung, C.; Burdick, J. A. *Advanced Drug Delivery Reviews* **2008**, *60*, 243–262.
(58) Bonaventure, J. *Experimental Cell Research* **1994**, *212*, 97–104.
(59) Raimondi, M. T.; Boschetti, F.; Falcone, L.; Fiore, G. B.; Remuzzi, A.; Marinoni, E.; Marazzi, M.; Pietrabissa, R. *Biomechanics and Modeling in Mechanobiology* **2002**, *1*, 69–82.
(60) Sharma, B.; Elisseeff, J. *Annals of biomedical engineering* **2004**, *32*, 148–159.
(61) Hu, J. C.; Athanasiou, K. A. *Tissue Engineering* **2006**, *12*, 969–979.
(62) Charles Huang, C. Y.; Reuben, P. M.; D'Ippolito, G.; Schiller, P. C.; Cheung, H. S. *Anat. Rec.* **2004**, *278A*, 428–436.
(63) Zhang, Z.; McCaffery, J.; Spencer, R.; Francomano, C. *Journal of Anatomy* **2004**, *205*, 229-237.
(64) Grogan, S. *Osteoarthritis and Cartilage* **2003**, *11*, 403–411.
(65) Martin, I.; Wendt, D.; Heberer, M. *TRENDS in Biotechnology* **2004**, *22*, 80–86.
(66) Pörtner, R.; Nagel-Heyer, S.; Goepfert, C.; Adamietz, P.; Meenen, N. *Journal of bioscience and bioengineering* **2005**, *100*, 235–245.
(67) Concaro, S.; Gustavson, F.; Gatenholm, P. *Bioreactor Systems for Tissue Engineering* **2009**, 125–143.
(68) Saini, S.; Wick, T. *Biotechnology progress* **2003**, *19*, 510–521.
(69) Vunjak Novakovic, G.; Martin, I.; Obradovic, M.; Treppo, S.; Grodzinsky, A.; Langer, R.; Freed, L. *Journal of Orthopaedic Research* **1999**, *17*, 130–138.
(70) Freed, L.; Marquis, J.; Langer, R.; Vunjak-Novakovic, G.; Emmanual, J. *Biotechnology and Bioengineering* **1994**, *43*, 605-614.
(71) Darling, E.; Athanasiou, K. *Tissue Engineering* **2003**, *9*, 9–26.
(72) Pei, M.; Solchaga, L.; Seidel, J.; Zeng, L.; Vunjak-Novakovik, G.; Caplan, A.; Freed, L. *The Journal of Federation of American Societies for Experimental Biology* **2002**, *16*, 1691-1694.
(73) Pazzano, D.; Mercier, K.; Moran, J.; Fong, S.; DiBiasio, D.; Rulfs, J.; Kohles, S.; Bonassar, L. *Biotechnology progress* **2000**, *16*, 893–896.
(74) Dunkelman, N.; Zimber, M.; LeBaron, R.; Pavelec, R.; Kwan, M.; Purchio, A. *Biotechnology and Bioengineering* **1995**, *46*, 299-305.
(75) Almarza, A. J.; Athanasiou, K. A. *Annals of biomedical engineering* **2004**, *32*, 2–17.
(76) Fithian, D.; Kelly, M.; Mow, V. *Clinical Orthopaedics and Related Research* **1990**, *252*, 19–31.
(77) Athanasiou, K.; Rosenwasser, M.; Buckwalter, J.; Malinin, T.; Mow, V. *Journal of Orthopaedic Research* **1991**, *9*, 330–340.
(78) Rudert, M. *Cells Tissues Organs* **2000**, *171*, 229–240.
(79) Mesa, J. M.; Zaporojan, V.; Weinand, C.; Johnson, T. S.; Bonassar, L.; Randolph, M. A.; Yaremchuk, M. J.; Butler, P. E. *Plastic and Reconstructive Surgery* **2006**, *118*, 41–49.
(80) Acosta, C.; Izal, I.; Ripalda, P.; Douglas-Price, A.; Forriol, F. *Journal of Orthopaedic Research* **2006**, *24*, 2087–2094.
(81) Lewis, P.; McCarty, L.; Yao, J.; Williams, J.; Kang, R.; Cole, B. *J Knee Surg* **2010**, *22*, 196–204.
(82) Mainil-Varlet, P.; Rieser, F.; Grogan, S.; Mueller, W.; Saager, C.; Jakob, R.

*Osteoarthritis and Cartilage* **2001**, *9*, S6–S15.
(83) Buschmann, M.; Gluzband, Y.; Grodzinsky, A.; Kimura, J.; Hunziker, E. *Journal of Orthopaedic Research* **1992**, *10*, 745–758.
(84) Petersen, J.; Ueblacker, P.; Goepfert, C.; Adamietz, P.; Baumbach, K.; Stork, A.; Rueger, J.; Poertner, R.; Amling, M.; Meenen, N. *Journal of Materials …* **2008**, *19*, 2029–2038.
(85) Kandel, R.; Grynpas, M.; Pilliar, R.; Lee, J.; Wang, J.; Waldman, S.; Zalzal, P.; Hurtig, M. *Biomaterials* **2006**, *27*, 4120–4131.
(86) Schulze-Tanzil, G.; Mobasheri, A.; de Souza, P.; John, T.; Shakibaei, M. *Osteoarthritis and Cartilage* **2004**, *12*, 448–458.
(87) Murphy, C.; Polak, J. *Journal of cellular physiology* **2004**, *199*, 451-459.
(88) Mandl, E.; Jahr, H.; Koevoet, J.; Van Leeuwen, J.; Weinas, H.;Verhaar, J.; van Osch, G. *Matrix biology* **2004**, *23*, 231-241.
(89) Tran-Khanh, N.; Hoemann, C.; McKee, M.; Henderson, J.; Buschmann, M. *Journal of Orthopaedic Research* **2005**, *23*, 1354–1362.
(90) Khan, A.; Suits, J.; Kandel, R.; Waldman, S. *Biotechnology progress* **2009**, *25*, 508–515.
(91) Khan, A. A.; Surrao, D. C. *Tissue Engineering Part C: Methods* **2011**, *ahead of print*.
(92) Lane, J.; Brighton, C.; Menkowitz, B. *The Journal of Rheumatology* **1977**, *4*, 334–342.
(93) Lee, R.; Urban, J. *Biochemical Journal* **1997**, *321*, 95-102.
(94) Waldman, S.; Couto, D.; Omelon, S. *Tissue Engineering* **2004**, *10*, 1633–1640.
(95) Xu, X.; Urban, J.; Browning, J.; Tirlapur, U.; Wilkins, R.; Wu, M.; Cui, Z. *Osteoarthritis and Cartilage* **2007**, *15*, 396-402.
(96) Wilkins, R.; Hall, A. *Journal of cellular physiology* **1995**, *164*, 474-481.
(97) Kuettner, K.; Pauli, B.; Gall, G.; Memoli, V.; Schenk, R. *The Journal of Cell Biology* **1982**, *93*, 743–750.
(98) Mishell, B.; Shiigi, S. *Selected methods in cellular immunology*; Freeman: San Francisco WP, 1980; p. 486.
(99) Bostrom, H.; Mansson, B. *The Journal of biological chemistry* **1952**, *196*, 483-488.
(100) Peterkofsky, B.; Diegelmann, R. *Biochemistry* **1971**, *10*, 988–994.
(101) Kim, Y.; Sah, R.; Doong, J.; Grodzinsky, A. *Analytical biochemistry* **1988**, *174*, 168-176.
(102) Qiu, W.; Murray, M.; Shortkroff, S.; Lee, C.; Martin, S. *Wound Repair and Regeneration* **2000**, *8*, 384–391.
(103) Lin, L.; Zhou, C.; Wei, X.; Hou, Y.; Zhao, L. *Arthritis Rheum* **2008**, *58*, 1067–1075.
(104) Hoch, D. H.; Grodzinsky, A. J.; Koob, T. J.; Albert, M. L.; Eyre, D. R. *Journal of Orthopaedic Research* **1983**, *1*, 4–12.
(105) Jin, H.; Lewis, J. *Journal of biomechanical engineering* **2004**, *126*, 138-146.
(106) Hayes, W.; Keer, L.; Herrmann, G.; Mockros, L. *Journal of biomechanics* **1972**, *5*, 541-551.
(107) Farndale, R.; Buttle, D.; Barrett, A. *Biochimica et Biophysica Acta (BBA)* **1986**, *883*, 173–177.
(108) Goldberg, R.; Kolibas, L. *Connective tissue research* **1990**, *24*, 265-275.
(109) Woessner, J. *Archives of biochemistry and biophysics* **1961**, *93*, 440-447.

(110) Brandt, K. D.; Doherty, M.; Lohmander, L. S. *Osteoarthritis*; Biochemistry and metabolism of normal and osteoarthritic cartilage; Oxford University Press, USA: New York, **1998**; pp. 74–84.
(111) Chevrier, A.; Rossomacha, E.; Buschmann, M. D.; Hoemann, C. D. *The Journal of Histotechnology* **2005**, *28*, 165-175.
(112) Weir, E.; Pretlow, T.; Pitts, A.; Williams, E. *Journal of Histochemistry & Cytochemistry* **1974**, *22*, 1135–1140.
(113) ICRS Cartilage Injury Evaluation Package. *www.cartilage.org*. **Accessed 2010.**
(114) Kunz, M.; Devlin, S.; Gong, R. H.; Inoue, J.; Waldman, S. D.; Hurtig, M.; Abolmaesumi, P.; Stewart, J. *Medical Image Computing and Computer-Assisted Intervention* **2009**, *5761*, 75–82.
(115) Ma, B.; Ellis, R. E. *Medical Image Analysis* **2003**, *7*, 237–250.
(116) Stockwell, R. *Journal of Anatomy* **1971**, *109*, 411–421.
(117) Waldman, S.; Grynpas, M.; Pilliar, R.; Kandel, R. *Journal of biomedical Materials Research* **2002**, *62*, 323-330.
(118) Mankin, H.; Mow, V.; Buckwalter, J.; Iannotti, J.; Ratcliffe, A. *Orthopaedic basic science*; Simon, S., Ed. Form and function of articular cartilage; American Academy of Orthopaedic Surgeons: Columbus, 1994; pp. 1–44.
(119) Hung, C. T.; Lima, E. G.; Mauck, R. L.; Taki, E.; LeRoux, M. A.; Lu, H. H.; Stark, R. G.; Guo, X. E.; Ateshian, G. A. *Journal of biomechanics* **2003**, *36*, 1853–1864.
(120) Lee, C.; Marion, N.; Hollister, S.; Mao, J. *Tissue Engineering Part A* **2009,** *15*, 3923-3930.
(121) *www.arthritis.org*. **Accessed 2011**
(122) Hunziker, E.; Switzerland, B.; Rosenberg, L. *The Journal of Bone and Joint Surgery* **1996**, *78*, 721–33.
(123) Richmond, J.; Hunter, D.; Irrgang, J.; Jones, M; Levy, B.; Marx, R.; Snyder-Mackler, L.; Watters, W.; Haralson, R.; Turkleson, C.; Wies, J.; Boyer, K.; Anderson, S.; Andre, J.; Sluka, P.; McGowan, R. *Journal of the Academy of Orthopaedic Surgeons* **2009**, *17*, 591-600.
(124) Adkisson, H., IV; Gillis, M.; Davis, E.; Maloney, W.; Hruska, K. *Clinical Orthopaedics & Related Research* **2001**, *391*, S280-S294.
(125) Yu, H.; Grynpas, M.; Kandel, R. A. *Biomaterials* **1997**, *18*, 1425–1431.
(126) Shapiro, F.; Koide, S.; Glimcher, M. *The Journal of Bone and Joint Surgery* **1993**, *75*, 532-553.
(127) Che, J.; Zhang, Z.; Li, G.; Tan, W.; Bai, X.; Qu, F. *Knee Surgery, Sports Traumatology, Arthroscopy* **2010**, *18*, 496–503.
(128) French, E.; VandeWoude, S.; Granowski, J.; Maul, D. Assessment of pain in laboratory animals. *www.colostate.edu/dept/lar/Pain_Assessment.doc.* **Accessed 2010**.
(129) Mankin, H. *The Journal of Bone and Joint Surgery. American Volume* **1982**, *64*, 460-466.
(130) Rahfoth, B.; Weisser, J.; Sternkopf, F.; Aigner, T.; Mark, Von Der, K.; Bräuer, R. *Osteoarthritis and Cartilage* **1998**, *6*, 50–65.
(131) Lorentzon, R.; Alfredson, H.; Hildingsson, C. *Knee Surg Sports Traumatol Arthrosc* **1998**, *6*, 202–208.
(132) Hurtig, M.; Fretz, P.; Doige, C.; Schnurr, D. *Canadian Journal of Veterinary*

*Research* **1988**, *52*, 137.
(133) Bruns, J.; Kersten, P.; Silbermann, M.; Lierse, W. *Arch Orthop Trauma Surg* **1997**, *116*, 66–73.
(134) Brittberg, M. *Clinical Orthopaedics and Related Research* **1999**, *367*, S147-S155.
(135) Furukawa, T.; Eyre, D.; Koide, S.; Glimcher, M. *Journal of Bone and Joint Surgery* **1980**, *62,* 1-11.
(136) Schreiber, R.; Ilten-Kirby, B.; Dunkelman, N.; Symons, K.; Rekettye, L.; Willoughby, J.; Ratcliffe, A. *Clinical Orthopaedics and Related Research* **1999**, *367*, S382-395.
(137) Grynpas, M.; Alpert, B.; Katz, I.; Lieberman, I.; Pritzker, K. *Calcified Tissue International* **1991**, *49*, 20-26.
(138) Buschmann, M.; Gluzband, Y.; Grodzinsky, A.; Hunziker, E. *Journal of Cell Science* **1995**, *108*, 1497–1508.
(139) Chua, K.; Aminuddin, B.; Fuzina, N.; Ruszymah, B. *Med J Malaysia* **2004**, *59B*, S7–S8.
(140) Lu, Y.; Adkisson, H.; Bogdanske, J. *The Journal of Knee Surgery* **2005**, *18*, 31–42.
(141) Waldman, S. D.; Usprech, J.; Flynn, L. E.; Khan, A. A. *Osteoarthritis and Cartilage* **2010**, *18*, 864–872.
(142) Nam, E. K.; Makhsous, M.; Koh, J.; Bowen, M.; Nuber, G.; Zhang, L. Q. *American Journal of Sports Medicine* **2004**, *32*, 308-316
(143) Mainil-Varlet, P.; Aigner, T.; Brittberg, M.; Bullough, P.; Hollander, A.; Hunziker, E.; Kandel, R.; Nehrer, S.; Pritzker, K.; Roberts, S.; Stauffer, R.; *Journal of Bone and Joint Surgery* **2003**, *85*, S45-57
(144) Brittberg, M.; Peterson, L.; Sjogren-Jansson, E.; Tallheden, T.; Lindahl, A.; *Journal of Bone and Joint Surgery* **2003**, *85*, S109-S115

# Appendix A: Continuous Flow Bioreactor


**Figure A 1** Set-up of the continuous flow bioreactor housed within the incubator

# Appendix B: Macroscopic and Histologic Scoring Sheets

## CARTILAGE REPAIR ASSESSMENT

| Criteria | Points | |
|---|---|---|
| Degree of Defect Repair<br>I Protocol A [1] | * In level with surrounding cartilage<br>* 75% repair of defect depth<br>* 50% repair of defect depth<br>* 25% repair of defect depth<br>* 0% repair of defect depth | 4<br>3<br>2<br>1<br>0 |
| I Protocol B [2] | * 100% survival of initially grafted surface<br>* 75% survival of initially grafted surface<br>* 50% survival of initially grafted surface<br>* 25% survival of initially grafted surface<br>* 0% (plugs are lost or broken) | 4<br>3<br>2<br>1<br>0 |
| II Integration to Border zone | * Complete integration with surrounding cartilage<br>* Demarcating border < 1mm<br>* 3/4 of graft integrated, 1/4 with a notable border >1mm width<br>* 1/2 of graft integrated with surrounding cartilage, 1/2 with a notable border > 1mm<br>* From no contact to 1/4 of graft integrated with surrounding cartilage | 4<br>3<br>2<br>1<br>0 |
| III Macroscopic Appearance | * Intact smooth surface<br>* Fibrillated surface<br>* Small, scattered fissures or cracs<br>* Several, small or few but large fissures<br>* Total degeneration of grafted area | 4<br>3<br>2<br>1<br>0 |
| Overall Repair Assessment | Grade I normal 12 P<br>Grade II nearly normal 11-8 P<br>Grade III abnormal 7-4 P<br>Grade IV severely abnormal 3-1 P | |

**Cartilage Biopsy** **Location** _____

| (1) Protocol A: | (2) Protocol B: |
|---|---|
| autologous chondrocyte implantation (ACI); periosteal or perichondrial transplantation; subchondral drilling; microfracturing; carbon fibre implants; others: | Mossaicplasty; OAT; osteochondral allografts; others: |

**Figure B 1 ICRS Cartilage Injury Evaluation System.** Macroscopic evaluation and scoring of each rabbit knee was determined using Protocol A of the repair assessment form. Based on the points received (0 to 12 points) they were given a repair Grade of I (normal) to IV (severely abnormal)[113].

**Table B 1** Histological grading scale for samples

| Histological Parameter | Score |
|---|---|
| I) Tissue morphology (viewed under polarized light) | *0% - full thickness collagen fibres*<br>*100% - normal cartilage birefringence* |
| II) Matrix staining | *0% - no staining*<br>*100% - full metachromasia* |
| III) Cell morphology | *0% - no round/oval cells*<br>*100% - mostly round/oval cells* |
| IV) Chondrocyte clustering (4 or more cells) | *0% - present*<br>*100% - absent* |
| V) Surface architecture | *0% - delamination or major irregularity*<br>*100% - smooth surface* |
| VI) Basal integration | *0% - no integration*<br>*100% - complete integration* |
| VII) Formation of a tidemark | *0% - no calcification front*<br>*100% - tidemark* |
| VIII) Subchondral bone abnormalities | *0% - abnormal*<br>*100% - normal (no infiltrates)* |
| IX) Inflammation | *0% - present*<br>*100% - absent* |
| X) Abnormal calcification/ossification | *0% - present*<br>*100% - absent* |
| XI) Vascularization (within the repair tissue) | *0% - present*<br>*100% - absent* |
| XII) Surface/superficial assessment | *0% - total loss or complete disruption*<br>*100% - resembles intact articular cartilage* |
| XIII) Mid/deep zone assessment | *0% - fibrous tissue*<br>*100% - normal hyaline cartilage* |
| XIV) Overall assessment | *0% - bad (fibrous tissue)*<br>*100% - good (hyaline cartilage)* |

# Appendix C: Distance Maps

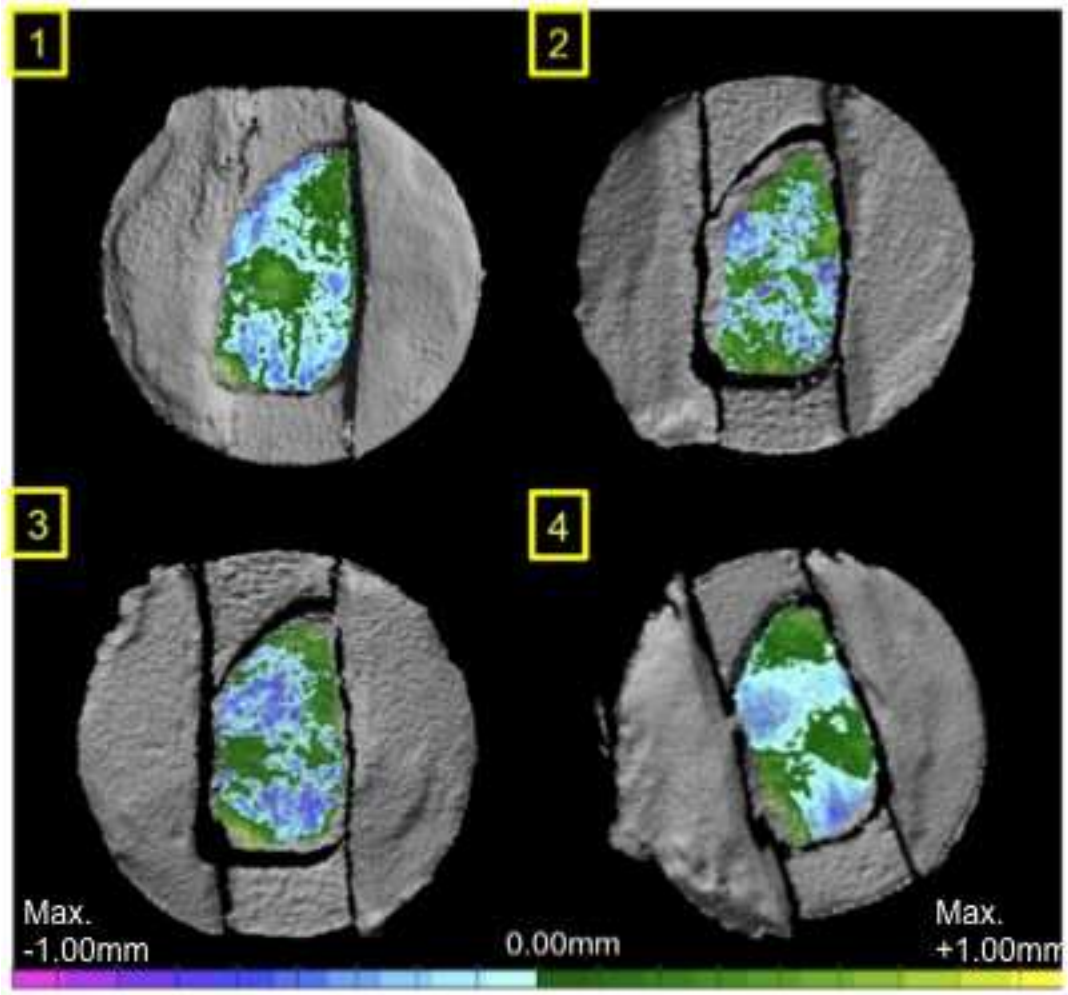


**Figure C 1 Distance map for each mold construct.** Surface geometry for the four constructs with an average RMS error of 114 ± 2 μm.

# Appendix D: IHC Stained Sections

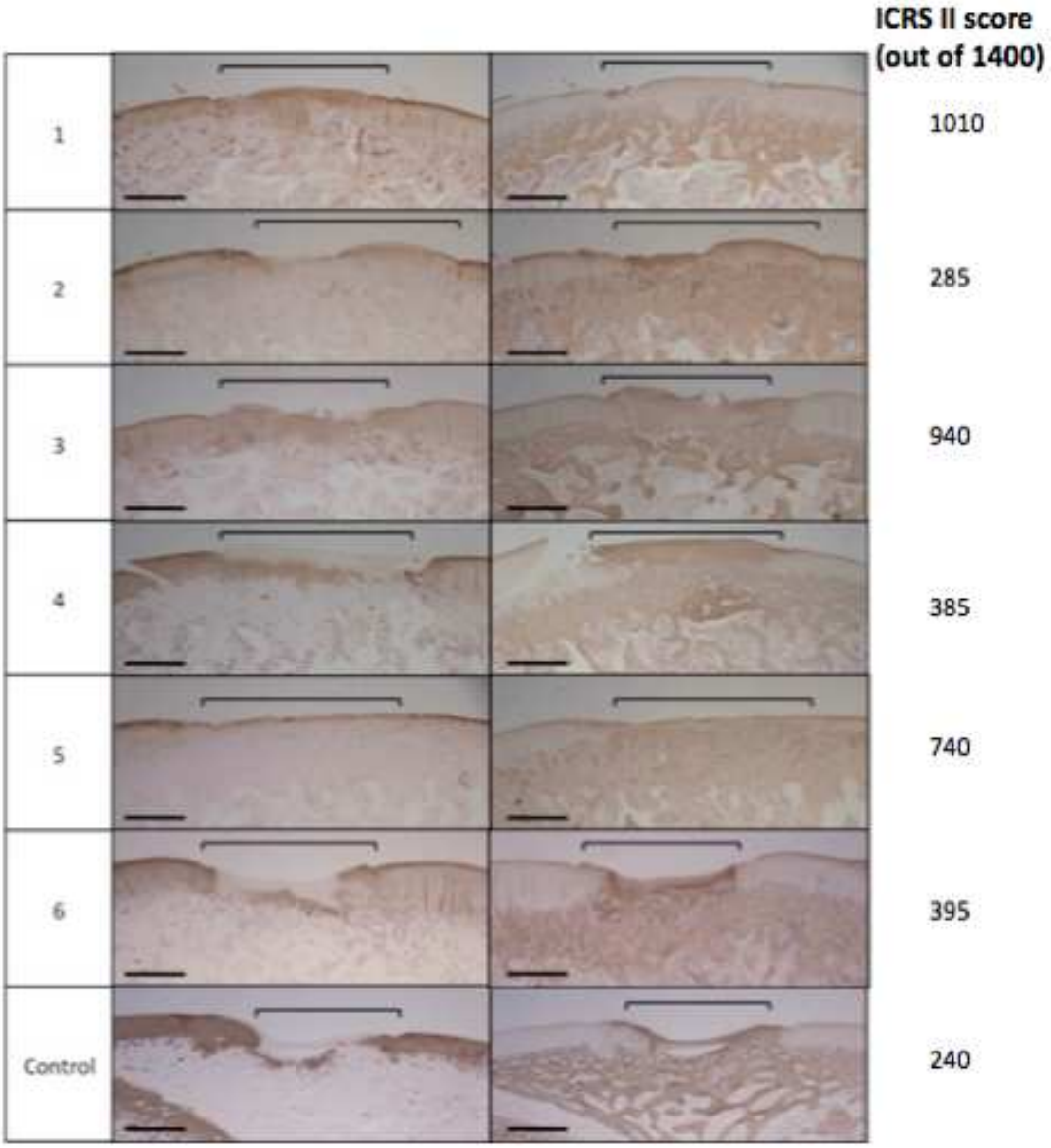


**Figure D 1** IHC staining of the 1 month treated defects and control for collagen II (left) and collagen I (right) at 1 month post-operatively. Defect area is outlined in black and ICRS II scoring on the right (scale bar: 100 μm).

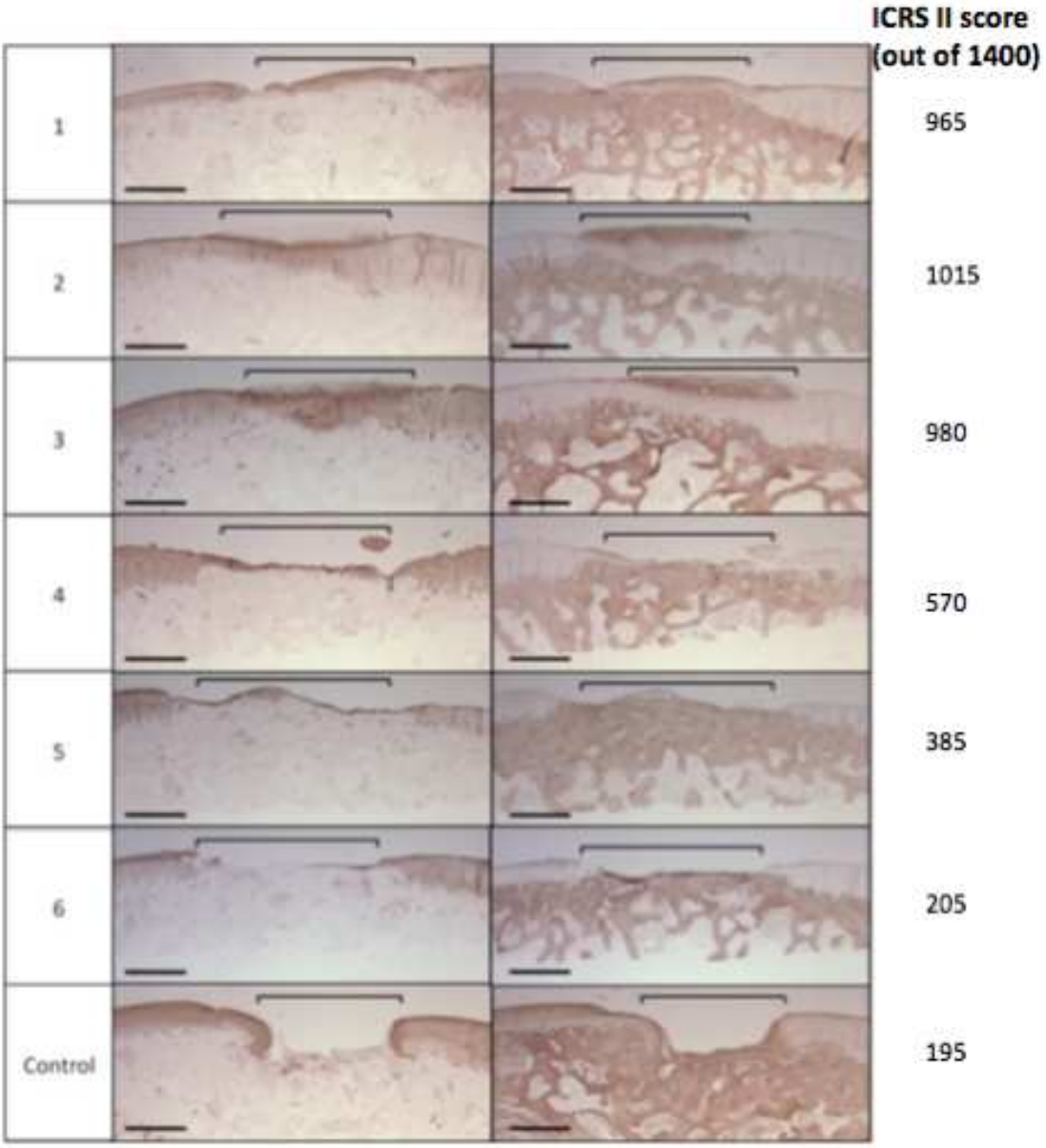


**Figure D 2** IHC staining of the 3 month treated defects and control for collagen II (left) and collagen I (right) at 3 months post-operatively. Defect area is outlined in black and ICRS II scoring on the right (scale bar: 100 μm).

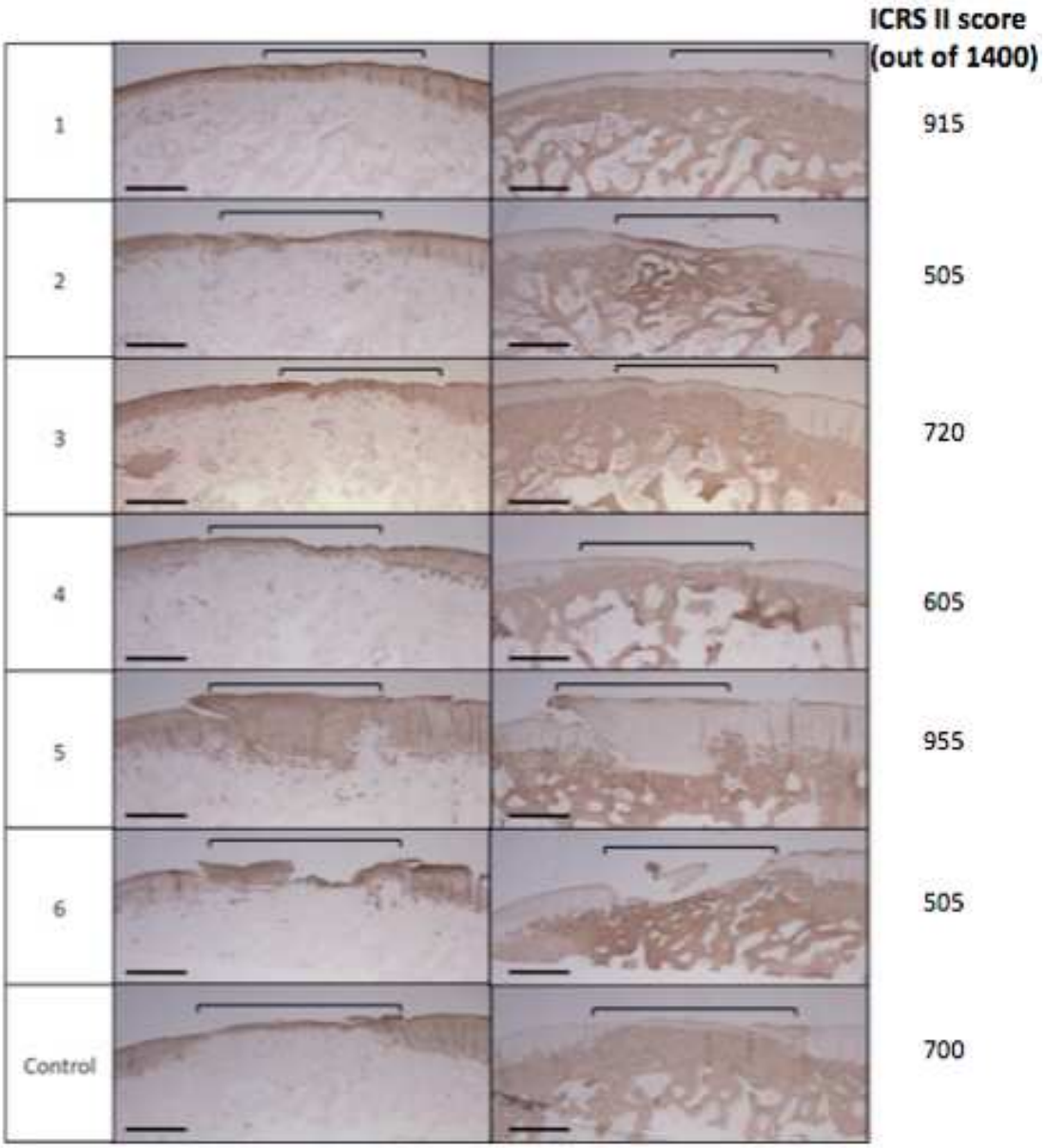


**Figure D 3** IHC staining of the 6 month treated defects and control for collagen II (left) and collagen I (right) at 6 months post-operatively. Defect area is outlined in black and ICRS II scoring on the right (scale bar: 100 μm).